Journal of African Earth Sciences 158 (2019) 103519

Contents lists available at ScienceDirect

Journal of African Earth Sciences

journal homepage: www.elsevier.com/locate/jafrearsci

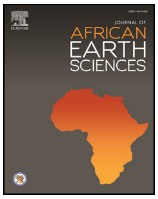

Spatial distribution and trace element geochemistry of laterites in Kunche area: Implication for gold exploration targets in NW, Ghana

Emmanuel Daanoba Sunkari[a,*], Michael Appiah-Twum[b], Abdurrahman Lermi[a]

[a] *Department of Geological Engineering, Faculty of Engineering, Niğde Ömer Halisdemir University, Main Campus, 51240, Niğde, Turkey*
[b] *School of Resource and Environment, University of Electronic Science and Technology of China, Qingshuihe Campus, No. 2006, Xiyuan Ave, West Hi-Tech Zone, 611731, Chengdu, Sichuan, China*

ARTICLE INFO

Keywords:
Laterite geochemistry
Duricrust
Pathfinder elements
Orogenic gold deposits
Ghana

ABSTRACT

Kunche area is located in NW Ghana within the Wa-Lawra greenstone Birimian belt and is composed mainly of volcaniclastics, metasediments and some intrusive granitoids. The area is covered with laterites making it difficult to identify exploration targets. In this study, we describe a new methodology based on statistical tools and trace element geochemistry to map the pathfinder elements of gold deposits in lateritic context. However, the results of this study are specific to a particular context and cannot be extrapolated without supplementary studies to all the lateritic areas. In this respect, a total of 67 lateritic samples were collected from residually weathered materials and their spatial distribution was determined by means of the GIS-based kriging interpolation method. The samples collected vary from detrital to residual laterites/duricrusts and are hosted in volcaniclastic rocks. ICP-MS and XRF techniques were used to determine the element concentrations of the samples. The trace element geochemical data were analyzed using bivariate and multivariate geostatistical analysis to establish relationships among elements. Fe-oxides such as goethite and hematite and clay minerals like kaolinite are the main secondary minerals of the concretionary reddish lateritic samples. All the analyzed elements showed asymmetrical distribution rather than normal distribution. Spearman correlation shows that Cu, Pb, S, As, and Ag have moderate to strong positive correlation with Au. From the multivariate geostatistical analysis, three element associations; a) Fe, Pb, S, Co, Cr; b) Ni, Y, Rb, Sr, Zn, and c) Ca, Cu, Mn, Ti, Zr, As, Au, Ag were observed. Threshold values of selected elements were determined using the median absolute deviation (MAD) method, which indicates possible anomalous concentrations in the laterites for Pb (≥48 ppm), Cu (≥46 ppm), As (≥134.2 ppm), and Ag (≥0.42 ppm). Multi-element mapping indicates that Pb + Cu + As + Ag is the most ideal association in the exploration of gold deposits. It reveals ellipsoidal anomalies comparable to the Au distribution map that suggest dispersion and accumulation of the pathfinder elements in the area. The geochemical anomalies are mainly restricted to the environment of the residual laterites in the Kunche area and we recommend that exploration programs should be focused in such areas.

1. Introduction

The term laterite is often used to describe indurated level (duricrust) present in some tropical regolith profiles (e.g., Arhin et al., 2015; Ilyas et al., 2016; Anand et al., 2019). Laterites are abundant with a widespread global distribution in many deeply weathered environments (Anand and Paine, 2002). Laterite materials and their mode of formation differ with some laterites forming in-place as residual products of weathering and others forming from a transported source (da Costa et al., 2016). Despite their different origins, both types of duricrusts have a similar orientation of chemistry. They are both poor in lessivable cations and mainly composed of Al/Fe oxides and more rare Al-rich clays. This is the direct result of their particular climatic conditions of formation, as they form in landscapes suffering a succession of extensive dry periods and short wet conditions (Aleva, 1994). Laterites are mainly formed as a result of secondary in situ cementation of unconsolidated materials overlying the parent bedrock (Taylor and Eggleton, 2001). Their formation generally depends on hydrology, topography and the primary rock. The formation of in situ duricrust is generally linked to the in situ accumulation of Fe/Al (Beauvais and Colin, 1993). It may result in iron oxide pisolith accumulation in the mottled zone and induration in the top of the profile (Nahon and Tardy, 1992). Recently, Chardon et al. (2018) opined that in West Africa, detrital duricrusts are often found covering lateritic pediments, which

---

[*] Corresponding author.
E-mail address: emmanueldaanoba.sunkari@mail.ohu.edu.tr (E.D. Sunkari).

https://doi.org/10.1016/j.jafrearsci.2019.103519
Received 19 September 2018; Received in revised form 29 May 2019; Accepted 3 June 2019

serve as obstacles to mineral exploration. The distribution of duricrusts on the landscape mainly depends on the past erosion, which translates into the present day by the local topography. However, laterite formation can also be the result of cementation of residual weathered materials as well as sediments from varied sources, hence their classification as residual and detrital laterites on the basis of origin (Anand et al., 2001). The lateritic pediments described by Chardon et al. (2018) have similar geomorphological characteristics with depositional environments in the Wa-Lawra greenstone Birimian belt in Ghana (Arhin et al., 2015). These environments characteristic of northern Ghana have gently inclined slopes of transportation and erosion that truncate the regolith and form at the confluence of eroding slopes and areas of sediment deposition (Arhin, 2013). Indurated and loose transported sediments are also common in the depositional environments of the Wa-Lawra greenstone Birimian belt as it was observed in the lateritic pediments area described by Chardon et al. (2018). During the period of secondary re-cementation in both in situ and detrital duricrusts, some elements behave as immobile elements due to changes in physico-chemical conditions causing unusual economical trace element enrichment such as detrital gold coatings on lithic units of clastic materials. The unusual enrichment of gold in such materials is because gold has an affinity for Fe-oxide, therefore, during the process of lateritization, gold grains may be coated to Fe-oxide (e.g., Freyssinet et al., 2005; Anand and Butt, 2010; Butt, 2016). Anand et al. (2001) documented erratic gold distributions in laterite capped areas in Australia. Butt and Bristow (2013) also documented auriferous laterite prevalence in the entire West African sub-region. Recently, Anand et al. (2019) reported auriferous ferricrete in the Yilgarn Craton of Western Australia and pointed out that the ferricrete gold deposits formed downslope of saprolite hills and are from proximal sources. However, the re-cemented unconsolidated units of different provenance identified in these studies appear erratic and thus, their elemental concentrations may not give a true representation of the underlying mineralization.

In such context, Anand (2001) and Cornelius et al. (2001) used several terminologies in describing iron coated lateritic materials (ferruginous materials). The authors mentioned that ferruginous duricrusts are regolith materials cemented by Fe regardless of their source. They are characterized by lateritic residuum (lateritic duricrust), ferricrete, and lateritic gravels (ferruginous lag) or a combination of all. The lateritic duricrust represents the ferruginous zone and occupies low rises, crests and mesas (Butt and Zeegers, 1992). As explained earlier, it forms as a result of ferruginization and residual accumulation of Fe and Al oxides as well as silica in the residual regolith. Depending on the formation conditions and materials, the lateritic duricrusts may have a uniform composition, which reflects the host rock lithology (Eggleton, 2001). Their chemical composition may still be similar due to the leaching/accumulation of geochemical elements from the host rocks. Ferricretes develop over/at the expense of sediments and have no distinguishable proximal bedrock source and thus, are sometimes considered to be of detrital origin (Anand et al., 2019). They may be reworked materials that originate from detrital sources with diverse jumbled materials and hence, could be termed detrital duricrusts (Cornelius et al., 2001). Accordingly, detrital duricrusts are formed as a result of cementation of sediments by Fe oxide impregnation with characteristics controlled by the nature of the matrix and cementing material (Anand, 1998). The matrix can be detrital clasts, sands and clays whereas the cementing material can be Fe-oxides, kaolinite, gibbsite, goethite and hematite. Ferruginous lag represents relics of Fe-rich regolith materials and varies depending on the degree of erosion and type of topography (Cornelius et al., 2001). It is generally composed of fragments of mottled saprolite, fragments of lateritic duricrust on hill crests, pisoliths and cutans on backslopes, and intercalations of polymictic materials in depositional (mixed) environments (Anand, 2001; Cornelius et al., 2001). In all, ferruginous duricrusts can be in situ or detrital in origin; when they come from in situ sources, they are simply referred to as lateritic duricrusts but if from detrital sources, they are generally known as detrital ferruginous duricrusts.

In the Wa-Lawra greenstone Birimian belt of Ghana, Arhin and Nude (2009) documented evidence of erratic gold distribution in the laterite dominated area. Identifying pathfinder elements of gold in such a complex regolith terrain is very difficult (Nude et al., 2012, 2014; Butt, 2016). Therefore, many workers have recognized laterites as the appropriate geochemical sample media for identifying pathfinder elements of gold in such terrains (Arhin, 2013; da Costa et al., 2016). The use of laterite trace element geochemistry in mineral exploration was initiated by Mazzucchelli and James (1966) in Western Australia and has since become a useful tool for successful gold exploration in the world (e.g., Anand et al., 2001; da Costa et al., 2016). By determining the behavior of trace elements in laterites within complex regolith environments, it is possible to completely understand secondary geochemical dispersion mechanisms useful for geochemical exploration programs (Arhin, 2013). Trace element associations in laterites can also point to where samples can be obtained and which type of sample to collect. Also, multi-element geochemistry stands as one of the best tools for delineating anomalies related to primary mineralization in tropical terrains covered by laterites and has been used by many researchers (e.g., Taylor and Thornber, 1992; Colin et al., 1993; Araújo, 1994; Marker et al., 1994; da Costa and Araújo, 1996). Since mineralization can be dispersed or concealed, laterally enhanced or diluted, delineating the actual anomaly using multi-element geochemistry is therefore worthwhile in geochemical exploration.

Kunche area in NW Ghana lies within the Wa-Lawra greenstone Birimian belt that is mainly composed of volcaniclastics, metasediments and some intrusive granitoids. The area is reported to have potential for gold mineralization associated with the volcaniclastics (Waller et al., 2012) but several attempts in harnessing and exploring for this valuable resource have been abortive over the years. Many exploration companies have since either abandoned their concessions or temporary halted their exploration activities in search for better ways of optimizing exploration. The exploration methods that were employed by the earlier exploration companies were adopted from those used in southern Ghana though the climates are different in both regions. The Kunche area is characterized by a savannah climate and such landscape is widely known to have abundant laterites and deeply weathered profiles (Butt and Zeegers, 1992). The regolith profiles of savannah areas are covered by very thick and consolidated ferruginous duricrust contrary to rainforest landscapes (Freyssinet, 1993). These variations in the landscape are usually due to modifications enhanced by climate, biological activities, topography, laterization, and thus, strictly require a different approach to interpreting element mobility and different exploration procedures. Southern Ghana has a homogenous regolith profile (Arhin, 2013) and gold (Au) is liberated from ore bodies in this area by chemical dissolution (Bowell, 1992). Au released by this process involves cyanide, fulvate, hydroxyl, and thiosulphate complexing and is re-precipitated via in-situ processes (Arhin, 2013). Accordingly, the mineralogy of Au in the regolith becomes complex. Also, the Au mineralogy in the regolith materials in southern Ghana is principally controlled by the prevailing physico-chemical processes during lateritic pedogenesis that led to in-situ and supergene Au mineralization (Arhin, 2013). Therefore, dispersion and mobilization mechanisms of elements in the savannah regions of Ghana like the Kunche area are different from the rainforest dominated southern parts. However, these geochemical processes are poorly known in the Kunche area since the mineralization is concealed by lateritic materials. This study seeks to identify the laterite types in Kunche area and to understand the nature of the underlying parent rocks using the trace element concentrations of the laterites complemented by multivariate geostatistical analysis. This information is used to determine areas of unusual element enrichment, the primary geological environment, and of the possible existence of base and precious metals mineralization, as there are few outcrops of primary rocks in the area. The study also aims at unravelling the distribution pattern of the pathfinder elements of gold and their

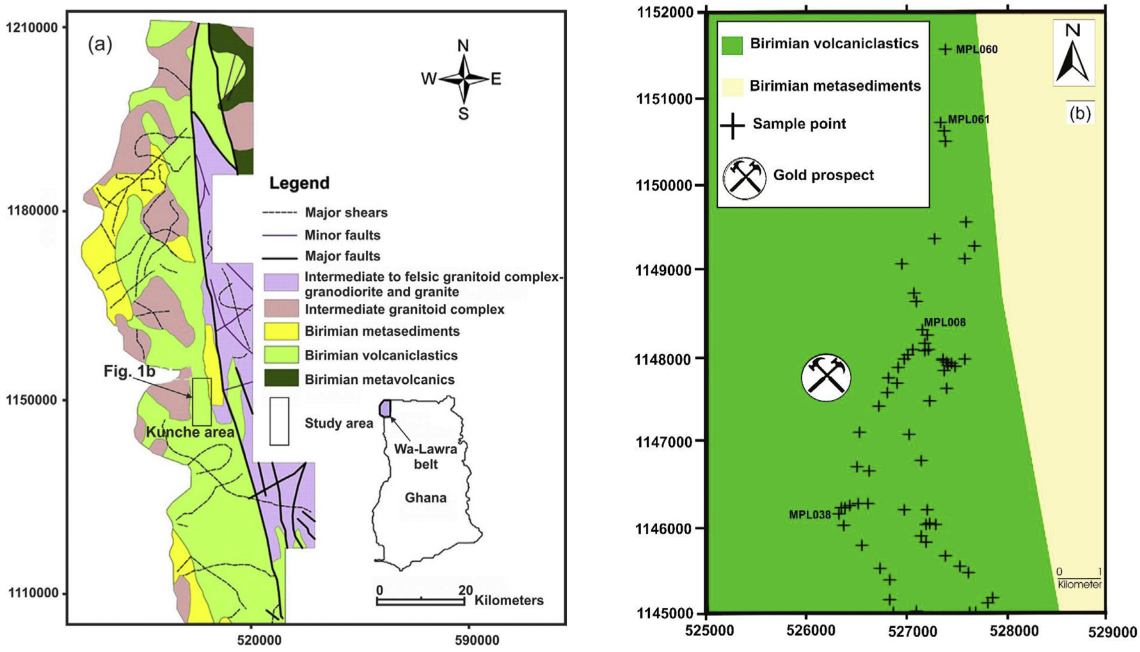

Fig. 1. (a) Geological map of the Wa-Lawra greenstone Birimian belt showing the dominance of Birimian volcaniclastics in Kunche area (after Arhin et al., 2015), and (b) Geological section of the Kunche area showing the sampling points and the contact between the Birimian volcaniclastics and metasediments.

geochemical associations, something not well understood in lateritic crusts.

2. Geological setting and gold mineralization

Kunche area is located in NW Ghana and forms part of the Wa-Lawra greenstone Birimian belt (Fig. 1a). Undifferentiated pyroclastic rocks, volcaniclastics, granitoids, metavolcanics, and metasedimentary rocks of the Birimian system (Kesse, 1985; Hirdes et al., 1992; Arhin and Nude, 2009; Nude et al., 2012; Sunkari and Zango, 2018) dominate the Wa-Lawra greenstone Birimian belt. However, in the Kunche area, the predominant lithologies are volcaniclastics, metasediments and some intrusive granitoids (Fig. 1a and b). There are minor occurrence (areal extent) of sedimentary rocks such as shales, slates, siltstones, dolostones, sheared conglomerates, greywackes, argillaceous rocks, and metamorphic rocks comprising phyllites and tuffaceous schists. They are fine to medium-grained and consist of thick isoclinally folded and steeply dipping alternating rock features (Arhin and Nude, 2009). The rocks are intruded by small, intermediate granitoids in some parts of Kunche with some unique fault and shear zones running through them (Fig. 1a). Laterites are abundant in most parts of Kunche with mature lateritic profiles occurring as hills and plateaus whereas immature lateritic profiles made of stripped regolith profiles (i.e. without duricrust) are only restricted to low-land areas. The laterites in the area developed within the mafic to intermediate lithologies with Fe–Mn oxides, kaolinite and smectite clays (within the saprolite) as principal secondary minerals (Arhin, 2013).

The mafic rocks in the area are highly weathered in the low-lying areas, especially those with high goethite and hematite content, which indicates typical weathering and decomposition under warm and humid climate. The depth and extent of weathering is not the same, it keeps changing from place to place. The regolith profile of the Kunche area begins with saprock and continues with saprolite, mottled zone, laterite zone, and an organic zone comparable to the observations of Arhin (2014) in the entire Wa-Lawra greenstone Birimian belt (Fig. 2). The regolith distribution is disorganized with extensive unusual sediment concealment intercalated with laterites as well as truncated surfaces at areas with saprolite either close to, or at the surface (Arhin and Nude, 2009; Arhin, 2014). The residual regolith materials are characteristically preserved at ridge tops and at moderately elevated settings. The proximal transported materials are found at the base of ridges and on pediments. Ferricretes are also common and are widespread in the area. They occur in depressions, low-lying areas, and sometimes near streams.

Prior to the discovery of gold mineralization in the Wa-Lawra greenstone Birimian belt in 1935, there were several small scale artisanal mining activities termed as “galamsey” in the area (Junner, 1935). However, mainstream feasibility exploration for gold in this part of Northern Ghana dates back to 1960 after a comprehensive geological mapping and prospecting by the Ghana Geological Survey in collaboration with the Soviet Union (Nude et al., 2012). Geochemical exploration started in 1990 which involved a regional scale stream sediment survey of the Wa-Lawra greenstone Birimian belt employing BLEG technique (Nude et al., 2012). The survey yielded substantial geochemical anomalies but when juxtaposed with anomalies in southern Ghana, the anomalies discovered in the Wa-Lawra belt were suggested to be economically not viable. Later between 1997 and 2000, a major geochemical survey was undertaken in the whole Wa-Lawra greenstone Birimian belt (Carter, 1997). Exploration works are still ongoing in the Wa-Lawra greenstone Birimian belt. Gold deposits in the Birimian greenstone belts of Ghana occur as mesothermal quartz vein mineralization (orogenic gold) hosted in metavolcanic and metasedimentary rocks (Kesse, 1985; Griffis et al., 2002; Allibone et al., 2004; Smith et al., 2016). The mineralized veins often feature medium to fairly dark grey quartz and commonly contain visible gold along with relatively abundant granular pyrite, arsenopyrite, chalcopyrite, minor sphalerite and galena (ore minerals), chlorite, tourmaline, ankerite, and calcite as gangue minerals (Dzigbodi-Adjimah, 1993; Amponsah et al., 2015). Locally, in the Kunche area, mineralization is related to an N–S to NNW-striking quartz vein system which contains mafic vein quartz and sulphides (Arhin, 2013). The veins are typically developed in a zone of interspersed wackes and phyllites known as the Kunche shear zone (Waller et al., 2012). The wackes are strongly brecciated as a result of shortening leading to deformation of the veins. But the brecciation textures are overprinted by planar shear fabrics throughout the mineralized zones (Waller et al., 2012). The deformed veins feature an alteration pattern consisting of silicification, sericitization, carbonitization, and chloritization (Amponsah et al., 2015).

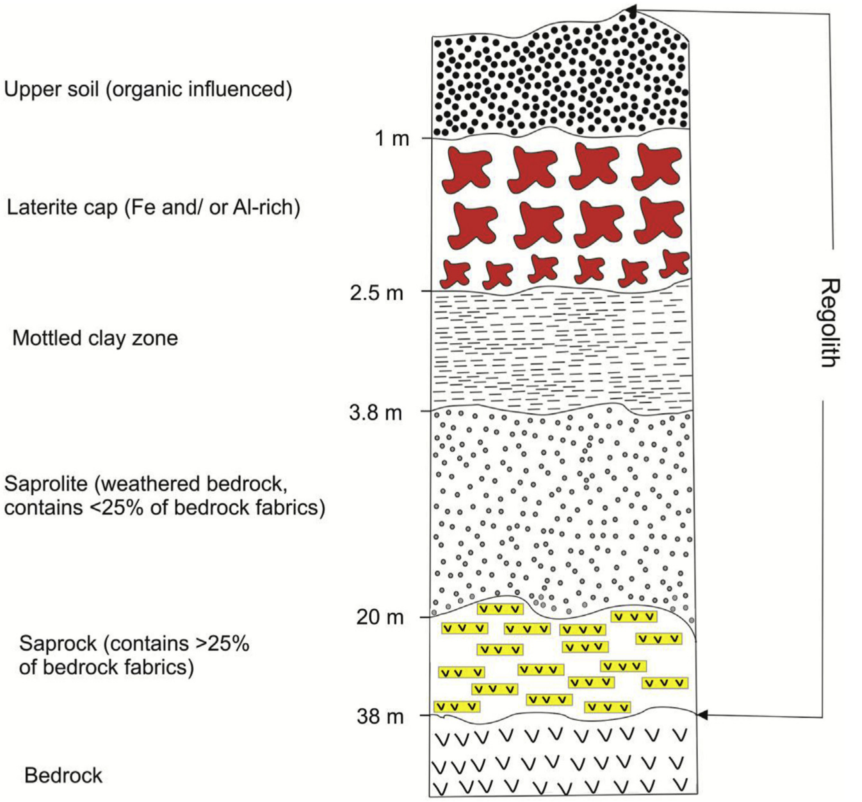

Fig. 2. Regolith profile of the Kunche area in the Wa-Lawra greenstone Birimian belt (modified from Arhin, 2014).

3. Sampling and analytical methods

3.1. Data acquisition

A total of sixty-seven (67) laterite samples were collected from a series of plateaus and hills in Kunche, NW Ghana in close proximity to a gold prospect (Fig. 1b). The laterite samples were collected from in-situ materials on the surface of the landscape, old pits, and from 30 cm diameter-holes dug in the plateaus and hills by means of a digging hoe. During the sampling, the first 20 cm was discarded since a large proportion of the area is covered by soils influenced in some places by organic substances. Lateritic materials ranging from a depth of 20–40 cm were collected from the dug holes as samples for the geochemical analysis. At each of the 67 sample points, 2 kg weight samples were collected and sent to the laboratory. To assure the quality control of the samples, replicate analyses of standards and duplicates were used based on the protocol of the geochemical laboratory of Azumah Resources Limited.

3.1.1. XRF analysis

X-Ray Fluorescence analysis (XRF) was conducted on the samples for their Fe, S, Mn, Ca, Ti, Cr, Mo, Ni, Co, Cu, Th, Rb, Sr, Zr, Y, Pb, Zn, and Sb contents at the geochemical laboratory of Azumah Resources Limited by means of a Panalytical Axios Advanced wavelength dispersive XRF. Prior to the analysis, each sample was separated into bulk (uncrushed sample), crushed form and pulverized form. The samples were dried overnight in a furnace at a temperature of 105 °C before fusion since laterites can easily absorb water from air. In order to minimize the matrix effects of the samples, the heavy absorber fusion technique of Norrish and Hutton (1969) was used for the trace element analysis. The fusion disk was made by mixing a 0.75 g equivalent of the roasted sample with 9.75 g of a combination of lithium metaborate and lithium tetraborate with lithium bromide as a releasing agent (Norrish and Hutton, 1969). Samples were later fused in Platinum (Pt) crucibles using an automated crucible fluxer and automatically poured into Pt molds for casting. The intensities were then measured and the concentrations calculated against the Ausmon standard which adjusted the calibration. Control standards were run to verify the procedure. The detection limits of all the analyzed elements are presented in Table 1. The values for Mo, Th, Zn, and Sb were however below the detection limit in most of the samples and are therefore not used in the geostatistical analysis.

3.1.2. ICP-MS

The As, Au, and Ag concentrations of the samples were determined by means of Inductively Coupled Plasma-Mass Spectrometry (ICP-MS). The samples were initially sieved to $< 125\,\mu m$ of c. 100 g each. 15 g of the samples were reacted with aqua regia (90 ml of 2-2-2) and subjected to leaching at 95 °C for 1 h, then the solution was diluted to 300 ml. The solution was filtered and analyzed by ICP-MS following the protocol of Eggins et al. (1997). The analysis yielded a detection limit of 5 ppb for Au and 0.01 ppm for Ag and As (Table 2).

3.2. Data processing

The mapped shape-features drawn from the collated information by means of Geographic Information System (GIS) software version 10.2.2 were draped onto the radiometric map of the area to produce a basic laterite map (1: 115000 scale) that indicates the various regolith regimes. By means of kriging interpolation method, the data obtained in the field was used to create a spatial distribution map of laterites in the Kunche area. The same method was used in generating contour maps for single and multi-element anomalies by means of surfer software version 13. It is a modern form of interpolation which operates through sub-setting and simulations of multiple variograms rather than single variograms (Sunkari et al., 2018).

Two-tailed Spearman correlation was used in measuring the linear association between two elements in a manner not influenced by the

Table 1
Trace element geochemical data of the lateritic samples in Kunche area, NW Ghana (Fe and S in %, Au in pbb, the rest in ppm; detrital duricrust refers to detrital ferruginous duricrust).

Sample ID	*X*	*Y*	*Laterite type/Env't*	*Fe*	*S*	*Mn*	*Ca*	*Ti*	*Cr*	*Mo*	*Ni*	*Co*	*Cu*	*Th*	*Rb*	*Sr*	*Zr*	*Y*	*Pb*	*Zn*	*Sb*	*As*	*Au*	*Ag*
MPL001	527374	1150607	Depositional environment	19.584	0.2937	270	243	1696	280	< 0.01	< 5	< 10	61	< 6	16.9	10.9	289	6.4	29	< 5	< 0.001	162	8	0.02
MPL002	527382	1150495	Depositional environment	21.0779	0.2603	261	1420	2392	331	3.7	< 5	< 10	35	21	18.5	52.7	281	4	24	< 5	< 0.001	96	82	0.01
MPL003	527595	1149553	Quartz pebbles	25.5074	0.2429	253	305	1570	321	< 0.01	< 5	< 10	205	21	19.6	14	167	4.4	27	< 5	< 0.001	171	115	0.8
MPL004	527671	1149269	Quartz pebbles	34.1762	0.3591	439	963	1931	537	< 0.01	< 5	259	40	< 6	28.5	18.7	219	< 1	49	< 5	< 0.001	141	25	0.15
MPL005	527584	1149122	Quartz pebbles	44.0964	0.4161	303	676	1758	351	3.1	< 5	832	59	< 6	21.5	32.6	191	2.3	74	< 5	0.003	103	74	0.02
MPL006	527269	1149361	Depositional environment	43.9806	0.4517	873	470	1961	352	3.6	< 5	708	48	33	23.3	36.1	246	5.6	75	< 5	< 0.001	99	56	0.01
MPL007	527071	1148726	Detrital duricrust	25.2203	0.3729	269	496	1848	441	3.2	< 5	< 10	26	< 6	20.5	23.6	234	4.3	36	< 5	< 0.001	115	60	0.04
MPL008	527153	1148297	Lateritic duricrust	30.6207	0.3533	273	609	2298	420	< 0.01	< 5	< 10	33	< 6	22.5	39.8	282	4	40	< 5	< 0.001	129	80	0.07
MPL009	527202	1148227	Lateritic duricrust	23.9433	0.2736	1439	708	1727	379	< 0.01	155	561	104	< 6	42.9	14.2	98	12.5	49	90	< 0.001	112	66	0.09
MPL010	527174	1148130	Detrital duricrust	27.9585	0.2707	754	918	2315	353	< 0.01	< 5	< 10	30	< 6	19.7	14.2	193	5.7	37	< 5	< 0.001	110	71	0.5
MPL011	527220	1148057	Detrital duricrust	24.1258	0.2234	672	533	1598	372	< 0.01	31	< 10	123	< 6	15.1	16	192	6.5	33	< 5	0.003	88	101	0.3
MPL012	527358	1147940	Detrital duricrust	23.6216	0.3289	4560	781	1455	478	< 0.01	78	637	60	< 6	18.6	14	83	10.1	51	< 5	< 0.001	71	44	0.05
MPL013	527367	1147821	Lateritic duricrust	43.4478	0.4531	1027	1258	1858	492	< 0.01	54	1569	411	< 6	24.9	20.3	178	6.5	71	13	< 0.001	68	180	0.9
MPL014	527397	1147608	Lateritic duricrust	43.6221	0.4248	1075	1400	1398	539	< 0.01	41	1197	72	< 6	25.6	8.9	63	5.7	70	23	< 0.001	40	95	0.1
MPL015	527228	1147457	Depositional environment	28.9177	0.312	395	716	1842	405	< 0.01	< 5	512	24	< 6	13.6	16.6	208	3.9	41	< 5	< 0.001	35	40	0.11
MPL016	527146	1146770	Depositional environment	32.3029	0.3443	222	556	1508	335	4	< 5	< 10	95	< 6	15.2	15.3	154	4.2	45	< 5	< 0.001	39	44	0.25
MPL017	527057	1148059	Detrital duricrust	24.4435	0.3723	315	558	2151	315	5.1	< 5	< 10	25	< 6	23.1	11.6	170	4.6	33	< 5	< 0.001	30	38	0.01
MPL018	527394	1147918	Detrital duricrust	20.3366	0.2142	270	722	2153	238	< 0.01	< 5	< 10	69	19	16.1	21.1	344	8.5	29	< 5	< 0.001	20	110	0.5
MPL019	527443	1147906	Detrital duricrust	11.3436	0.2371	293	433	1632	226	< 0.01	< 5	< 10	20	19	8.4	13.4	216	6	11.2	< 5	< 0.001	18	22	0.04
MPL020	527486	1147862	Detrital duricrust	48.0384	0.3938	522	377	2116	426	3.8	< 5	2158	12	31	22.7	10.7	176	< 1	100	< 5	< 0.001	52	28	0.06
MPL021	527574	1147946	Depositional environment	23.2609	0.3195	239	484	2658	266	< 0.01	< 5	< 10	19	< 6	14.5	12.8	243	3	32	< 5	< 0.001	17	18	0.02
MPL022	527180	1148052	Depositional environment	29.4309	0.3425	478	715	2529	347	< 0.01	< 5	< 10	27	23	23.5	18.5	226	6.9	44	< 5	< 0.001	36	26	0.12
MPL023	527002	1147996	Depositional environment	42.1884	0.4124	348	836	2227	433	< 0.01	< 5	602	37	25	35.7	18.2	268	3.6	66	< 5	< 0.001	37	32	0.7
MPL024	526967	1147952	Depositional environment	24.7103	0.3296	247	638	1793	405	< 0.01	< 5	< 10	46	< 6	15.6	8.9	220	4.1	22	< 5	< 0.001	213	190	0.9
MPL025	526907	1147854	Depositional environment	26.6645	0.3761	250	1061	2428	405	< 0.01	< 5	< 10	30	23	17.7	72	239	< 1	26	< 5	< 0.001	125	96	0.65
MPL026	526812	1147730	Depositional environment	26.5562	0.262	286	412	1105	556	< 0.01	< 5	< 10	14	< 6	10.6	7.8	72	< 1	18	< 5	< 0.001	137	88	0.45
MPL027	526897	1147665	Depositional environment	28.7035	0.6572	404	1628	1877	641	< 0.01	< 5	< 10	19	< 6	24.4	69	172	3.5	34	< 5	< 0.001	168	130	0.73
MPL028	526807	1147560	Depositional environment	47.5032	0.4336	346	789	1653	672	< 0.01	< 5	< 10	21	< 6	11.9	28.8	99	< 1	42	< 5	< 0.001	93	113	0.4
MPL029	526720	1147399	Depositional environment	31.7506	0.4246	578	604	1809	371	< 0.01	< 5	287	26	33	14.6	21.2	156	< 1	27	< 5	< 0.001	89	56	0.05
MPL030	526519	1147100	Depositional environment	22.2325	0.3092	326	657	1978	446	< 0.01	< 5	< 10	23	< 6	17.3	18.3	208	3.1	19	< 5	< 0.001	116	77	0.3
MPL031	526504	1146694	Detrital duricrust	31.4538	0.3772	584	535	1457	631	< 0.01	167	< 10	131	< 6	27.3	6.3	65	1.02	35	129	< 0.001	127	101	0.75
MPL032	526614	1146641	Detrital duricrust	51.4071	0.4191	1328	996	2382	771	< 0.01	< 5	741	82	< 6	19.5	10.1	198	3	67	< 5	< 0.001	199	110	0.1
MPL033	526609	1146272	Lateritic duricrust	40.3218	0.3498	638	976	1737	528	< 0.01	< 5	552	70	< 6	14.9	8.9	145	3.5	41	< 5	< 0.001	100	55	0.02
MPL034	526509	1146264	Detrital duricrust	35.31	0.3775	744	700	1189	651	< 0.01	< 5	< 10	48	25	12.8	9	62	4.5	38	< 5	< 0.001	67	28	0.01
MPL035	526423	1146239	Detrital duricrust	55.2887	0.4212	559	942	1533	634	< 0.01	62	1528	39	< 6	18.3	9.2	89	< 1	76	91	< 0.001	42	24	0.05
MPL036	526379	1146220	Detrital duricrust	45.299	0.4176	309	905	1083	439	< 0.01	70	1371	30	< 6	20	10.8	66	10	71	74	< 0.001	43	13	0.02
MPL037	526345	1146218	Lateritic duricrust	31.5666	0.2695	356	829	1259	743	< 0.01	< 5	609	19	< 6	11.7	8.6	135	< 1	30	< 5	0.003	34	18	0.04
MPL038	526320	1146148	Detrital duricrust	21.9809	0.2313	137	359	623	289	< 0.01	< 5	< 10	14	< 6	6.4	9.4	99	< 1	23	< 5	< 0.001	17	22	0.04
MPL039	526973	1146198	Depositional environment	28.98	0.3432	297	441	1848	353	< 0.01	< 5	< 10	24	< 6	16.8	8.7	147	3.7	30	< 5	< 0.001	29	15	0.1
MPL040	527197	1146199	Depositional environment	25.8572	0.2606	236	609	1957	328	< 0.01	< 5	< 10	46	32	12.5	17.1	241	5.2	30	< 5	< 0.001	16	20	0.7
MPL041	527185	1146028	Depositional environment	8.8536	0.152	243	471	1507	240	< 0.01	< 5	< 10	8	22	4.3	6.2	197	2.6	3.9	< 5	< 0.001	12	17	0.01
MPL042	527232	1146029	Detrital duricrust	59.7008	0.4779	200	526	1617	550	< 0.01	< 5	1101	< 1	< 6	18.7	4.7	81	< 1	91	< 5	0.003	46	13	0.04
MPL043	527282	1146026	Detrital duricrust	20.9185	0.305	301	868	1836	355	< 0.01	< 5	< 10	16	< 6	10.3	7.3	133	< 1	18	< 5	< 0.001	13	22	0.01
MPL044	527145	1145892	Detrital duricrust	52.8647	0.5212	458	958	1337	538	4.4	< 5	< 10	66	< 6	22.1	13.6	147	7.5	76	< 5	< 0.001	61	28	0.46
MPL045	527185	1145818	Detrital duricrust	42.7512	0.3595	332	1003	1524	791	3.7	< 5	< 10	19	< 6	14.2	7.9	116	< 1	57	< 5	< 0.001	37	21	0.31
MPL046	527390	1145660	Detrital duricrust	58.1744	0.4047	583	1100	973	1704	< 0.01	62	< 10	88	< 6	20.5	6.5	56	11.1	66	61	0.004	48.1	16	0.07
MPL047	527531	1145533	Detrital duricrust	9.8867	0.2467	563	2749	1773	352	< 0.01	< 5	< 10	17	< 6	8	19	91	< 1	5	< 5	< 0.001	39	15	0.04
MPL048	527617	1145459	Detrital duricrust	13.731	0.2667	324	656	1420	484	< 0.01	< 5	2399	16	29	16.2	10.1	138	3.4	9	< 5	< 0.001	123	78	0.5
MPL049	527859	1145164	Depositional environment	28.2435	0.3162	328	703	1692	723	< 0.01	< 5	< 10	17	< 6	18.1	12.7	134	< 1	22	< 5	0.003	138	19	0.3
MPL050	527811	1145106	Depositional environment	25.6659	0.347	1857	1332	2601	272	5.2	< 5	< 10	26	< 6	20.5	39	292	6.7	55	< 5	< 0.001	77	121	0.04
MPL051	527684	1144995	Depositional environment	40.2693	0.3894	4520	927	2160	274	< 0.01	< 5	< 10	20	< 6	20.9	24.9	103	< 1	43	< 5	< 0.001	93	182	0.02
MPL052	527629	1144998	Depositional environment	10.8671	0.1836	480	1365	2750	359	< 0.01	< 5	< 10	18	31	24.2	43	174	4.6	13	31	< 0.001	46.1	124	0.66
MPL053	527089	1145006	Lateritic duricrust	29.0631	0.376	919	553	1832	471	< 0.01	70	1794	80	< 6	25.8	6.8	91	8.6	28	50	< 0.001	147	196	0.9
MPL054	526859	1145000	Lateritic duricrust	40.8079	0.4058	764	1153	3068	973	< 0.01	< 5	< 10	22	< 6	24.3	13.5	204	6.1	62	< 5	< 0.001	34	112	0.35

(*continued on next page*)

Table 1 (*continued*)

Sample ID	*X*	*Y*	*Laterite type/Env't*	*Fe*	*S*	*Mn*	*Ca*	*Ti*	*Cr*	*Mo*	*Ni*	*Co*	*Cu*	*Th*	*Rb*	*Sr*	*Zr*	*Y*	*Pb*	*Zn*	*Sb*	*As*	*Au*	*Ag*
MPL055	526822	1145143	Lateritic duricrust	19.5527	0.3288	932	1387	2319	415	3.2	40	935	26	23	25.2	14	174	5.4	19	16	< 0.001	19.5	74	0.15
MPL056	526820	1145378	Lateritic duricrust	39.3995	0.3945	215	925	3167	291	0.43	< 5	1275	14	< 6	17.6	9.5	248	< 1	49	< 5	< 0.001	< 0.01	28	0.02
MPL057	526724	1145512	Erosional environment	14.0496	0.2085	467	784	2132	587	< 0.01	< 5	989	13	< 6	10.3	7.9	109	2.7	8	< 5	< 0.001	21.4	12	0.04
MPL058	526550	1145774	Erosional environment	0.5994	0.3782	< 5	748	567	74	2	71	621	144	< 6	1.7	2.8	5.5	< 1	< 2	45	< 0.001	33	18	0.01
MPL059	526361	1146013	Erosional environment	5.5308	0.1529	534	1081	1157	329	< 0.01	< 5	350	< 1	< 6	5.5	5.9	82	2.9	6	28	< 0.001	4.2	11	0.02
MPL060	527384	1151571	Erosional environment	8.17	0.1621	669	1122	1458	309	< 0.01	< 5	< 10	< 1	< 6	10	7.6	85	< 1	5	23	< 0.001	12	24	0.01
MPL061	527334	1150706	Erosional environment	23.8861	0.3215	375	1208	1543	931	< 0.01	< 5	< 10	37	< 6	10	15	132	3.6	23	19	< 0.001	27	22	0.02
MPL062	526952	1149067	Erosional environment	20.7863	0.2543	205	275	1265	443	< 0.01	< 5	< 10	12	< 6	8.4	4.1	77	< 1	21	< 5	< 0.001	19	10	0.01
MPL063	527094	1148626	Erosional environment	12.7505	0.242	585	912	3420	642	< 0.01	89	< 10	56	19	48.8	8	146	8.6	13.4	36	< 0.001	66	36	0.7
MPL064	527020	1147072	Lateritic duricrust	46.0857	0.4912	595	1076	1631	1027	< 0.01	< 5	243	81	< 6	17.3	5.1	47	6.9	54	< 5	< 0.001	143	148	0.98
MPL065	527057	1148058	Lateritic duricrust	8.2692	0.19	639	2507	2038	388	< 0.01	29	274	36	< 6	34.2	35.8	192	11.1	6	37	< 0.001	40	46	0.34
MPL066	527358	1147948	Lateritic duricrust	29.2493	0.4036	577	514	2372	511	< 0.01	< 5	548	32	< 6	19.7	8.4	199	3.4	29	< 5	< 0.001	144	105	0.62
MPL067	527410	1147879	Detrital duricrust	19.3899	0.2607	381	877	2215	610	< 0.01	65	1087	39	24	21.5	9	133	3.5	18	6	< 0.001	107	168	0.84

measurement units (Davis, 1986). Quantile-quantile (Q-Q) plots were used to test normal distributions of the dataset of elements since the data may show some departure of the individual datasets from normality. Centered log-ratio (clr) transformation was applied to the geochemical data in this study to reduce the difference between the minimum and maximum concentrations prior to Principal Component Analysis (PCA) (Aitchison, 1986; Aitchison and Greenacre, 2002; Muriithi, 2015) using the expression:

$$\mathrm{clr}(x) = (\log(x_1/g(x)), \ldots, \log(x_N/g(x))) \tag{1}$$

where x represents the composition vector, g(x) is the geometric mean of the composition x, and x_1, x_2,..x_N are the concentrations of the individual elements. The significance of Principal Component Analysis (PCA) and Factor Analysis (FA) in this study was a linear transformation of original variables into a smaller number of uncorrelated latent variables. Hierarchical Cluster Analysis (HCA) was used to group the trace elements into clusters based on the similarity (or dissimilarity) of their chemical properties.

In recent years, the most commonly used statistical parameter for determining the threshold that separates the background value from the anomaly is the median absolute deviation (Teng et al., 2010; Yaylalı-Abanuz, 2013). The median absolute deviation method of Tukey (1977) was used to calculate the threshold values for delineating gold anomalies in the study area. The following formula was used;

$$T = \mathrm{med} + 2\mathrm{MAD} \tag{2}$$

where T is the anomaly threshold, med is the median value of the analyzed elements, and MAD is the median absolute deviation. The MAD is a measure of the dispersion of data and stands out as the best statistical measure of variability of a univariate sample of quantitative data (Tukey, 1977). It is calculated using the equation;

$$\mathrm{MAD} = \mathrm{median}\ |xi - \mathrm{median}\ (xi)| \tag{3}$$

where xi is the element concentration.

Single element mapping using the MAD abetted in delineating geochemical anomalies with respect to Au, Pb, Cu, As, and Ag. However, geochemical halos around mineral deposits can be delineated more efficiently with a combination of two or more pathfinder elements rather than a single element by a method called "multi-element halos technique" (Beus and Grigorian, 1977; Reis et al., 2001). By applying this technique, the threshold values for the multi-element halos were calculated using the formula;

$$H_{(X+Y)} = (X_1/X_0 + Y_1/Y_0); (X_2/X_0 + Y_2/Y_0); \ldots\ldots\ldots\ldots\ldots\ldots\ldots\ldots\ldots (X_N/X_0 + Y_N/Y_0) \tag{4}$$

where X_1, X_2, …, X_N are median values of X in samples 1, 2, …, N; Y_1, Y_2, …, Y_N are concentrations of Y in samples 1, 2, …, N; and X_0 and Y_0 are threshold (equation (2)) values of X and Y elements.

4. Results

4.1. Laterite types

Observations from old pits and surface materials in the laterite-capped Kunche area show that overlying the bedrock are pisoliths, quartz pebbles with ferricrete, clay units, and some rock fragments (Fig. 3). The pisoliths contain Fe-oxyhydroxides and the rock fragments encountered in some places on the surface are signatures of the up-shooting of the primary rocks mainly mafic volcaniclastics.

4.1.1. Lateritic duricrust (residual laterites)

Thirty-three percent (33%) of the laterites in the mapped area was identified to be of lateritic duricrust (residual laterites) classification (Fig. 4a). They are exposed in relict environments in the Kunche area, on high rises and hills (Fig. 3a). They also form with inclusions of

Table 2
Summary statistics of raw (untransformed) trace element concentrations of the lateritic samples (A.BC[a] – Average Basalt Composition; A.AC[a] - Average Andesite Composition).

Element	Fe[a]	S[a]	Mn	Ca	Ti	Rb	Sr	Zr	Y	Cr	Ni	Co	Cu	Pb	Zn	As	Au[a]	Ag
Detection limits	0.01	0.01	5	5	5	1	1	5	1	10	5	10	1	2	5	0.01	5	0.01
No. of samples	67	67	66	67	67	67	67	67	48	67	15	28	64	66	17	66	67	67
Mean	29.2	0.34	624.56	851.31	1846.36	18.53	16.81	160.01	5.4	479.75	72.27	919.25	50.31	37.81	45.41	75.07	63.24	0.26
Minimum	0.6	0.15	137	243	567	1.7	2.8	5.5	1.02	74	29	243	8	3.9	6	4.2	8	0.01
Maximum	59.7	0.66	4560	2749	3420	48.8	72	344	12.5	1704	167	2399	411	100	129	213	196	0.98
Median	27.96	0.34	399.5	781	1809	18.3	12.8	156	4.55	420	65	724.5	31	33	36	63.5	44	0.1
Standard Deviation	13.42	0.09	765.9	441.18	543.96	8.2	13.91	71.94	2.6	238	39.94	571.09	58.74	22.69	33.52	52.3	50.82	0.3
Sample Variance	180	0.01	586608	194637	295894	67	193.41	5174	6.65	56641	1595	326147	3450	514	1123	2735	2583	0.09
Skewness	0.25	0.4	4.29	2.05	0.39	1.02	2.3	0.22	1	2.46	1.55	1.04	4.19	0.65	1.17	0.65	1	1
Confidence Level (95.0%)	3.27	0.02	188.28	107.61	132.68	2	3.39	17.55	0.75	58.05	22.12	221.45	14.67	5.58	17.23	12.86	12.4	0.07
MAD	7.62	0.07											15.00	15.00		37.60	19.24	0.16
Threshold (median + 2MAD)	43.20	0.41											46.00	48.00		134.20	82.48	0.42
A.BC**	8.65	0.03	1500	76000	13800	30	465	140	21	170	130	48	87	6.0	105	2.0	4.0	0.11
A.AC**	5.85	0.02	1200	46500	8000	100	800	260	30	50	55	10	35	15	72	2.4	4.5	0.07

[a] Fe, S are % and Au is ppm; Average Basalt Composition** (Turekian and Wedepohl, 1961); Average Andesite Composition** (Vinogradov, 1962).

toughened indurated pisolithic units of ferruginous weathering remnants from underlying rocks. These laterites are made up of equigranular matrix materials within their structure, mainly clasts of Fe-oxide cemented colluvial and alluvial sediments with a uniform textural framework. The lateritic duricrusts are compact and hard (Fig. 3b). The lithic units contained in these laterites in the Kunche area comprise of quartz pebbles, pisoliths, and clay materials (Fig. 3c). Associated minerals identified with the lateritic duricrusts by means of hand lens in the field include Fe-oxides (goethite and hematite). The goethites identified in the field associated with the lateritic duricrusts are black nodular components that appear as pigments on the laterite matrix. The hematite minerals observed in the lateritic duricrusts show evidence of pre-existing joints in the outcrop that must have been infiltrated by water with time thereby weakening the joints and causing a further detachment of fragments from the parent laterite block (Fig. 3b). However, these descriptions are constrained by the lack of a robust analytical technique for the mineralogy. The classification of the lateritic duricrusts in the Kunche area is corroborated by evidence of similarities in angularities of the lithic units as well as the equal grain sizes and shape of matrix materials in relation to the pisoliths and saprolite materials overlying the bedrock in the regolith profile (Fig. 3d).

4.1.2. Detrital ferruginous duricrust (detrital laterites)

The detrital ferruginous duricrusts are outcropped and encountered at depositional environments. Sixty-seven percent (67%) of the duricrusts in the mapped area in Kunche were identified to be detrital ferruginous duricrusts (detrital laterites, Fig. 4a). They are distinguished by their equigranular nodules and heterogeneous internal fabrics of litho-relics and crop out in low rises, on steep hills and close to terrains of lateritic residuum in the Kunche area. Unique forms are found within a few centimeters below the surface of the regolith (Fig. 3e) and in some exposures of old pits (Fig. 3f). It seems a secondary organic-rich soil horizon was developing at the top of the duricrust level. The detrital ferruginous duricrusts also form as slabs and patches of different duricrust blocks cemented together by clay minerals. These laterites are made of some slightly equigranular and polymitic matrix materials (quartz pebbles, pisoliths, and Fe-oxide coatings) (Fig. 3g). The detrital ferruginous duricrusts have a non-uniform framework but less compact and less hard as compared to the lateritic duricrusts (Fig. 3h). The lithic units associated with them comprise of quartz pebbles, pisoliths, and rock fragments (volcaniclastics) (Fig. 3i). The detrital ferruginous duricrusts are also composed of Fe-oxides just as the lateritic duricrusts. The goethites here also seem to have black nodular features that appear as pigments on the laterite matrix as in the lateritic duricrusts. The detrital ferruginous duricrusts in the Kunche area also form from different jumbled materials from diverse sources (Fig. 3j).

Substantial portion of the mapped area was overlain by pisoliths that are cemented to form detrital laterites of varied texture and composition. This portion is classified as depositional environment (mixed environment) within the mapped area (Fig. 4a).

4.2. Trace element geochemistry

The trace element concentrations in the laterites are given in Table 1 whereas the summary statistics are presented in Table 2. There are large variations among the dataset thus, from clr transformation, this constraint was offset by reducing the variation between minimum and maximum concentrations using ratios between elements (Table 3). The raw concentrations of Fe, S, Mn, Ca, Ti, Cr, Co, and Zr vary from 1500 to 4560 ppm, Ni, Cu, Rb, Sr, Y, Pb, and Zn are in the range of 1.02 and 411 ppm whilst As, Au, and Ag changed from 0.01 to 213 ppm (Table 1). The concentrations of Fe (0.60–59%), S (0.15–0.66%), Mn (137–4560 ppm), Ti (567–3420 ppm), Cu (8.00–411 ppm), Ni (29–167 ppm), Pb (3.90–100 ppm), As (4.20–213 ppm), Au (8–196 ppb), and Ag (0.01–0.98 ppm) are higher in the lateritic duricrust than the detrital ferruginous duricrust (Table 1). Similar trend was observed even after the clr transformation (Table 2). The concentrations of Pb and As are also higher in the residual laterites than the detrital laterites (Table 1). Co, Rb, Sr, Zr, Y, and Zn have variable compositions in the detrital and residual laterites.

4.3. Geostatistical analysis of the chemical data

4.3.1. Spearman's correlation

The elements of interest in this analysis include S, Cu, Pb, Zn, As, Au, and Ag based on the mineralogy of the deposits in the area and their patterns may indicate possible mineralization in the study area especially in the environment of the residual laterites/duricrusts rather than the detrital laterites/duricrusts. The relationships amongst these elements are presented in a two-tailed Spearman correlation matrix in Table 4. S displays positive correlation (r = 0.23) with Au (Table 4). Similarly, Cu displays positive correlation (r = 0.31) with Au (Table 4). Pb shows a weak positive correlation (r = 0.11) with Au (Table 4). Zn however has negative correlation (r = −0.26) with Au (Table 4). Interestingly, As and Ag display similar good positive correlations with Au (r = 0.59) and (r = 0.58), respectively (Table 4). The positive correlation between these elements and Au particularly As and Ag may indicate a geochemical anomaly for gold from the perspective of exploration geochemistry. The rest of the elements show strong to weak

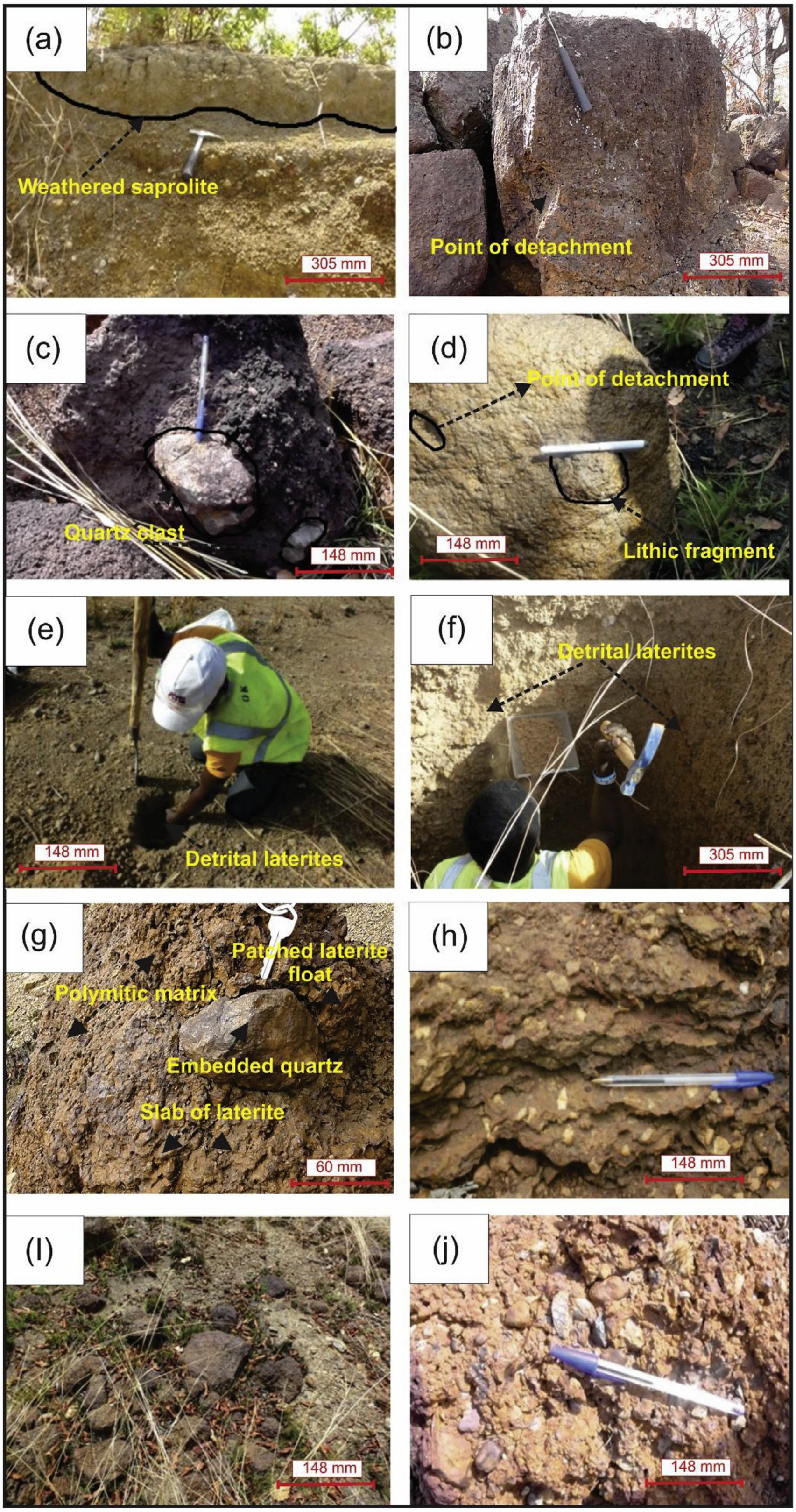

Fig. 3. (a) Laterite profile exposing the weathered saprolite and residual laterites in Kunche area (b) Lateritic duricrust showing points of detachment during weathering, (c) Lateritic duricrust with quartz clasts, (d) Lateritic duricrust with uniform composition and some clasts, (e) Detrital ferruginous laterites observed in a hole dug at 30 cm deep, (f) Detrital ferruginous laterites exposed in an old pit, (g) Detrital ferruginous duricrust formed from different jumbled materials, (h) Ferricrete with Fe-oxide coated sediments, quartz clasts, pisoliths and eroded ferruginous fragments, (i) Detrital ferruginous duricrust in the Kunche area with non-uniform composition, and (j) Eroded ferruginous fragments with pisoliths and quartz pebbles.

positive correlations with Au. The elements that are anti-correlated with gold suggest that the geochemical mobilization of these elements is unrelated to gold mineralization or they may have formed in association with gold but later remobilized due to complex geochemical processes.

4.3.2. *Quantile-quantile plots*

The quantile-quantile plots (Fig. 5) of the elements of interest fit well with normal distribution except at the higher values. This suggests that the geochemical data is normally distributed and those that appear not to be part of the normal distribution are outliers and may be points of mineralization.

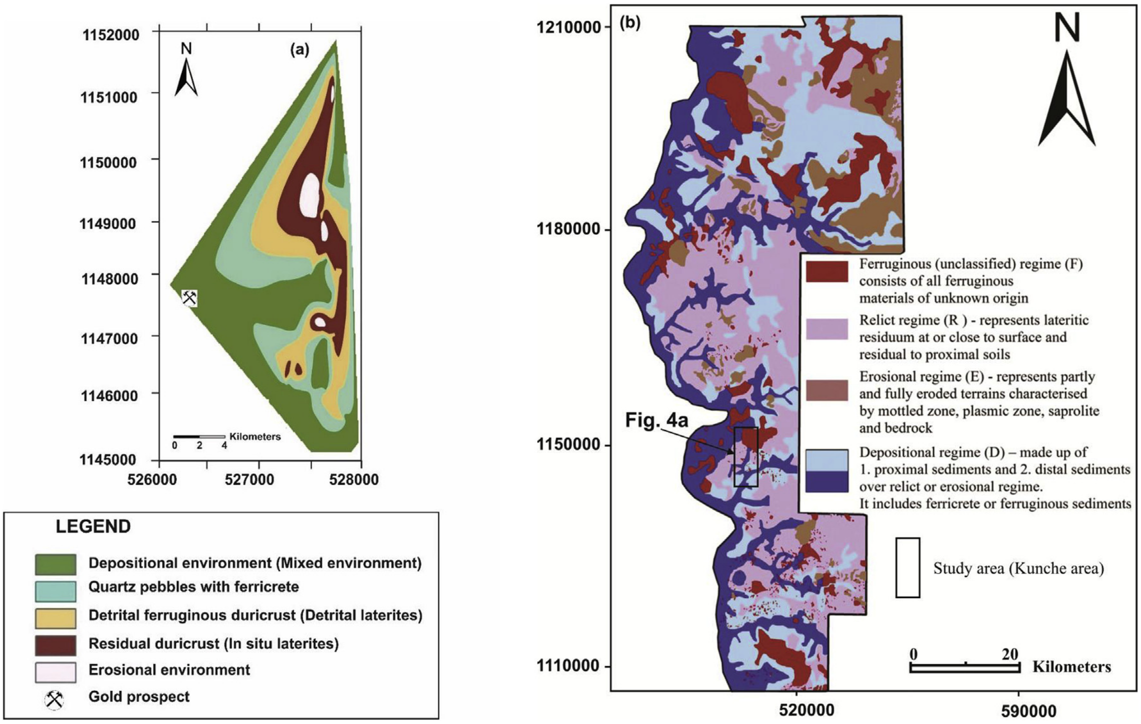

Fig. 4. (a) Spatial distribution of the laterite types in Kunche area. Depositional environment (mixed environment) is composed of pisoliths cemented to form detrital laterites whilst erosional environment depicts residual accumulations of weathered materials, and (b) Regolith map of the Wa-Lawra greenstone Birimian belt (after Arhin et al., 2015).

4.3.3. *Principal component analysis and factor analysis*

The principal component analysis using the untransformed data reveals three element associations involving (1) Fe, S, Pb (2) Mn, Cu, Co, Cr, Ni, Ti, As, Au, Ag (3) Ca, Rb, Sr, Zr, Y, Zn elements (Table 5; Fig. 6a). Similarly, the transformed data show slight variation with three element associations (1) Fe, S, Pb, Co, Cr; (2) Ni, Y, Rb, Sr, Zn and (3) Ca, Cu, Mn, Ti, Zr, As, Au, Ag (Table 5; Fig. 6b). The factor analysis also revealed that 76.770% of total variance of the untransformed data with initial eigenvalues > 3 relative to three components consists of all the elements in the above three element associations (Table 6), whereas a slightly lower variation (65.237%) of the transformed dataset accounts for the three element associations. Hence, the results of the factor analysis corroborates well with the results of the principal component analysis.

4.3.4. *Hierarchical cluster analysis*

The hierarchical cluster analysis presented in the form of a dendrogram for the untransformed data shows four clusters. Firstly, Fe, Pb, S, Co, and Cu cluster together (Fig. 7a). Cr, As, Au, and Ag also form the second cluster, Ca, Sr, Ti, and Zr constitute the third cluster whilst Mn, Ni, Rb, Y, and Zn make up the fourth cluster (Fig. 7a). The transformed data show three clusters (Fe, Pb, S, Co, Cr-cluster 1; Ni, Y, Rb, Sr, Zn-cluster 2; Ca, Cu, Mn, Ti, Zr, As, Au, Ag-cluster 3) on a dendrogram (Fig. 7b), comparable to the results of the PCA and FA.

4.4. *Geochemical anomalies*

Threshold values obtained from the median absolute deviation (MAD) method applied to Fe, S, Pb, Cu, As, Au, and Ag elements (elements associated with gold mineralization) are presented in Table 2. Comparing the threshold values in Table 2 to the element concentrations in Table 1 for both laterite types, it can be established that laterites with Fe, S, Pb, Cu, As, Au, and Ag concentrations above 27.10%, 0.41%, 48.00 ppm, 46.00 ppm, 134.20 ppm, 82.48 ppb and 0.42 ppm, respectively, are considered to be anomalous. This is because Tukey (1977) suggested that if the concentrations of some elements are above calculated threshold values using the MAD method, those concentrations define the anomalies in an area. Contour diagrams for single elements defined by the threshold values for Au, Pb, Cu, As, and Ag elements using the MAD method reveal similar ellipsoidal anomalies that denote dispersion and accumulation of the pathfinder elements around the northeastern, central and southeastern parts of Kunche in close proximity to the gold prospect in the area (Fig. 8a–e).

The multi-element mapping involving Fe + S + Cu, Fe + S + Pb + As, and Pb + Cu + As + Ag also resulted in ellipsoidal anomalies in the contour maps comparable to the single element

Table 3
Summary statistics of centered log-ratio transformed (clr) concentrations of the trace elements.

Element	Fe	S	Mn	Ca	Ti	Rb	Sr	Zr	Y	Cr	Ni	Co	Cu	Pb	Zn	As	Au	Ag
No. of samples	67	67	66	67	67	67	67	67	48	67	15	28	64	66	17	66	67	67
Mean	0.05	−1.45	0.004	0.003	0.002	0.07	0.07	0.01	0.13	0.01	0.02	0.003	0.03	0.04	0.03	0.02	0.03	−3.83
Minimum	−0.001	−2.4	0.003	0.003	0.001	0.01	0.03	0.01	0.002	0.004	0.02	0.003	0.02	0.02	0.02	0.01	0.01	−7.69
Maximum	0.06	−0.54	0.01	0.004	0.002	0.09	0.11	0.02	0.20	0.01	0.03	0.004	0.05	0.05	0.05	0.03	0.04	−0.03
Median	0.05	−1.37	0.004	0.003	0.002	0.07	0.07	0.01	0.12	0.005	0.03	0.003	0.03	0.04	0.03	0.02	0.03	−3.85
Standard Deviation	0.010	0.38	0.001	0.0002	0.0001	0.01	0.02	0.002	0.04	0.0004	0.003	0.0003	0.01	0.01	0.01	0.005	0.01	2.61
Sample Variance	0.00	0.00	0.00	0.00	0.00	0.00	0.00	0.00	0.002	0.00	0.00	0.00	0.00	0.00	0.00	0.00	0.00	6.83
Skewness	−2.68	−0.55	1.32	0.08	−0.98	−1.51	0.50	−2.27	−0.33	−0.31	0.36	−0.13	0.71	−0.90	−0.36	−0.57	−0.04	−0.0

Table 4
Two-tailed Spearman correlation matrix of selected elements (p ≤ 0.05; correlation coefficients ≥0.70 are highlighted in bold).

	Fe	S	Mn	Ca	Ti	Rb	Sr	Y	Cr	Ni	Co	Cu	Pb	Zn	As	Au	Ag
Fe	**1.00**																
S	**0.84**	**1.00**															
Mn	0.17	0.22	**1.00**														
Ca	0.04	0.13	0.47	**1.00**													
Ti	−0.05	0.02	0.10	0.20	**1.00**												
Rb	0.34	0.39	0.43	0.23	0.46	**1.00**											
Sr	0.04	0.08	0.06	0.22	0.49	0.34	**1.00**										
Y	0.11	0.07	0.37	0.20	−0.06	0.37	0.13	**1.00**									
Cr	0.47	0.40	0.30	0.28	−0.16	0.22	−0.24	−0.01	**1.00**								
Ni	−0.09	0.04	−0.04	−0.58	−0.18	0.22	−0.51	0.07	0.19	**1.00**							
Co	0.25	0.16	−0.16	−0.19	−0.01	0.12	−0.12	−0.05	0.10	−0.10	**1.00**						
Cu	0.26	0.28	0.36	0.10	−0.15	0.36	0.02	0.35	0.09	0.27	−0.15	**1.00**					
Pb	**0.88**	**0.79**	0.24	0.06	0.00	0.44	0.13	0.28	0.25	0.07	0.33	0.41	**1.00**				
Zn	0.35	0.21	−0.05	−0.55	−0.40	0.18	−0.28	0.43	0.08	0.53	0.05	0.24	0.34	**1.00**			
As	0.32	0.35	0.16	−0.07	0.14	0.42	0.22	−0.03	0.33	0.50	0.00	0.35	0.20	0.36	**1.00**		
Au	0.16	0.23	0.35	0.19	0.37	0.47	0.39	0.03	0.13	−0.16	0.10	0.31	0.11	−0.26	0.59	**1.00**	
Ag	0.14	0.10	0.12	0.10	0.21	0.42	0.13	0.15	0.37	−0.11	−0.01	0.28	0.01	−0.14	0.45	0.58	**1.00**

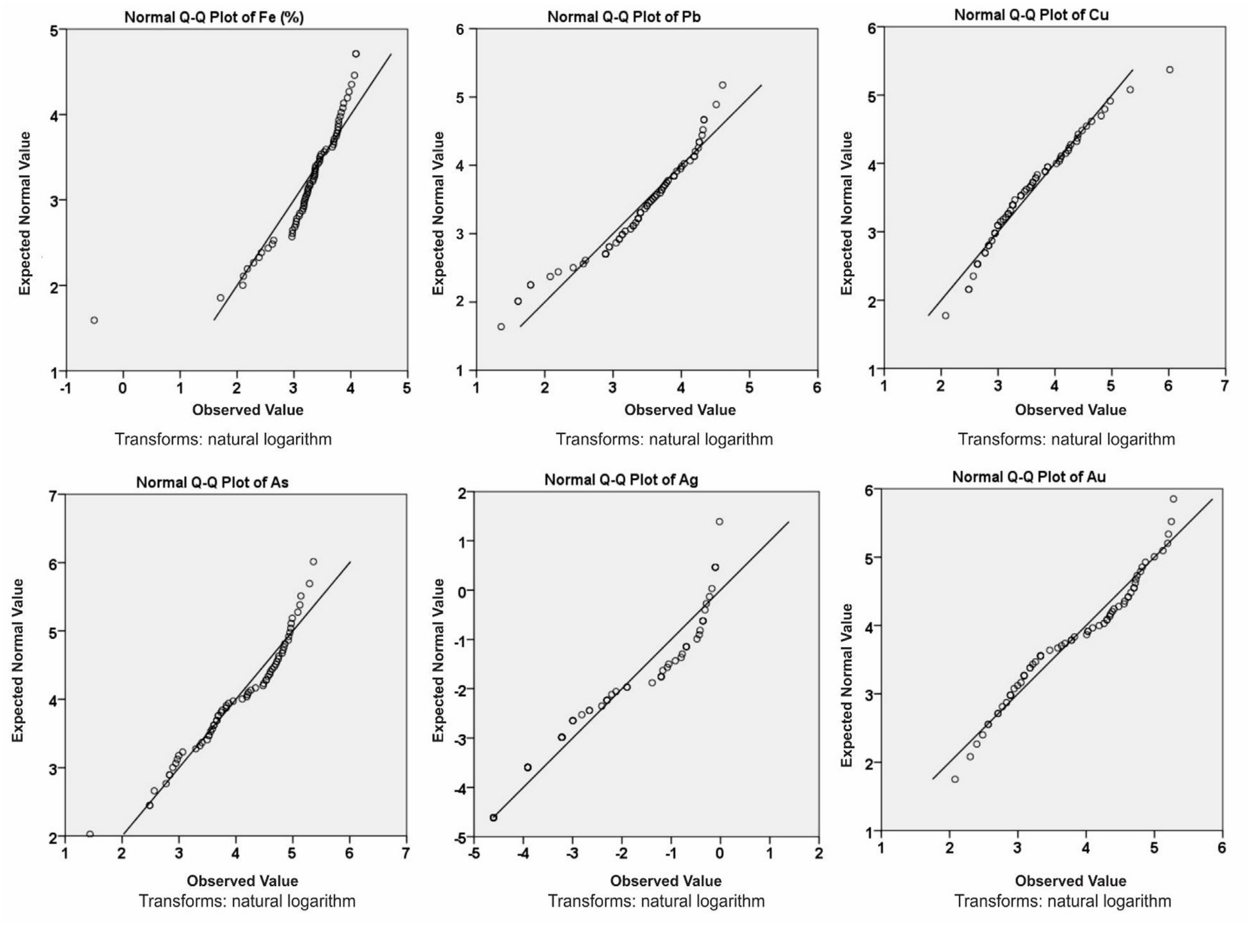

Fig. 5. Q-Q plots for Fe, Pb, Cu, As,Ag, and Au.

mapping (Fig. 9a, b, c). The Pb + As + Cu + Ag map appears to be the most homogenous one when compared with the Au distribution map. To confirm these anomalies and to understand whether the anomalies are significantly impacted by the lithology of the mafic host rocks, a multi-element ratio (Pb + As + Cu + Ag)/Zr contour diagram (Fig. 9d) was prepared using their raw concentrations in the supplementary table. It is observed in this diagram that the anomalies are mainly restricted to laterites with trace elemental ratios ranging from 2 to 2.4 hosted in volcaniclastic rocks (Fig. 9d). They fall in the same terrain with the contours using the element concentrations and median + 2MAD (Fig. 8a–e).

5. Discussion

5.1. Formation of the laterites

The information gathered from the laterite mapping in the field showed that the study area is largely composed of detrital ferruginous duricrusts (detrital laterites) and lateritic duricrusts (residual laterites) (Fig. 4a). The pisoliths and quartz pebbles associated with these type of

Table 5
Rotation component matrix (C1, C2 and C3 are the extracted components for both the raw and transformed data; strong positive loadings are in bold).

	Untransformed Component			Clr Transformed Component		
	C1	C2	C3	C1	C2	C3
Fe	**0.95**	0.11	−0.14	**0.96**	0.01	0.00
S	**0.86**	0.24	−0.23	**0.99**	−0.06	0.11
Mn	0.00	**0.56**	0.04	0.09	0.21	**0.39**
Ca	−0.53	−0.57	0.01	−0.34	−0.38	**−0.19**
Ti	−0.86	**0.36**	−0.14	−0.60	−0.51	**0.35**
Cr	0.21	**0.67**	−0.45	**0.29**	−0.81	0.07
Ni	0.15	**0.64**	0.05	0.14	0.31	0.03
Co	**0.64**	**0.65**	−0.18	**0.84**	−0.35	0.22
Cu	0.16	**0.38**	−0.04	0.36	0.08	**0.71**
Rb	−0.42	−0.35	**0.75**	−0.53	**0.55**	0.17
Sr	−0.63	−0.50	0.14	−0.51	0.33	0.10
Zr	−0.78	−0.34	0.01	−0.55	−0.26	**0.35**
Y	−0.03	−0.57	**0.69**	−0.14	**0.99**	0.10
Pb	**0.89**	−0.06	0.03	**0.88**	0.15	−0.06
Zn	0.29	−0.44	**0.80**	0.06	**0.94**	−0.08
As	−0.04	**0.69**	**0.65**	−0.09	0.02	**0.56**
Au	−0.08	**0.97**	−0.05	−0.02	−0.60	**0.69**
Ag	−0.25	**0.87**	−0.12	−0.29	−0.53	**0.80**

Extraction Method: Principal Component Analysis.
Rotation Method: Varimax with Kaiser Normalization.
a. Rotation converged in 6 iterations.

laterites are interpreted as transported detrital fragments overlying the regolith whilst the clay units are interpreted as remnants of residual laterites/duricrusts. However, the pisoliths found in the mottled zone suggest that the ones in the in situ duricrusts also have an in situ origin. The residual laterites/duricrusts formed as a result of residual accumulation and cementation of Fe-oxides and clay mineral concentrates through ferruginization. They are generally compact and hard with equigranular matrix materials having a uniform textural framework, consistent with the descriptions of Anand (2001) and Cornelius et al. (2001). In the Kunche area, erosion appears to be intense with truncated profiles in most places (Arhin, 2013). The truncation is high in the saprolite-dominated areas with kaolinite as the most important secondary mineral. A significant portion of the study area is truncated close to the base of pre-existing profiles where rock-forming silicates are the dominant minerals. These minerals have been oxidized by Fe-rich anoxic pore waters (Loder et al., 1978) thus, accounting for the presence of Fe-oxides in the residual laterites/duricrusts. With respect to the regolith profile (Fig. 2), the detrital ferruginous duricrusts in the Kunche area form the ferruginous zone and occur in transition zones between relict environments and depositional environments (Fig. 4a). This may imply that the depositional environments are Quaternary and the detrital ferruginous duricrust areas are older depositional environments. The detrital ferruginous duricrusts also developed over in situ duricrusts implying that they are younger than the in situ duricrusts. Evidence of differences in angularities of the lithic units, presence of slabs of laterite patches signifying composite accumulations as well as the uneven grain sizes and morphology of the matrix materials validate their classification as detrital ferruginous duricrusts according to the classification scheme of Anand (2001). The presence of the pisoliths in the laterites indicates nearness to a duricrust exposure whether uphill, downslope or an underlying laterite cap in the regolith profile. Indeed, the pisoliths were probably formed as a result of pedologic processes within the tropical regolith terrain of the Kunche area. A fraction of the mapped area showed evidence of erosion via truncation of the regolith profile and has been classified as erosional environment. The spatial distribution map of laterites in the study area (Fig. 4a) is consistent with the regolith map (Fig. 4b) of the entire Wa-Lawra greenstone Birimian belt earlier on studied by Arhin et al. (2015).

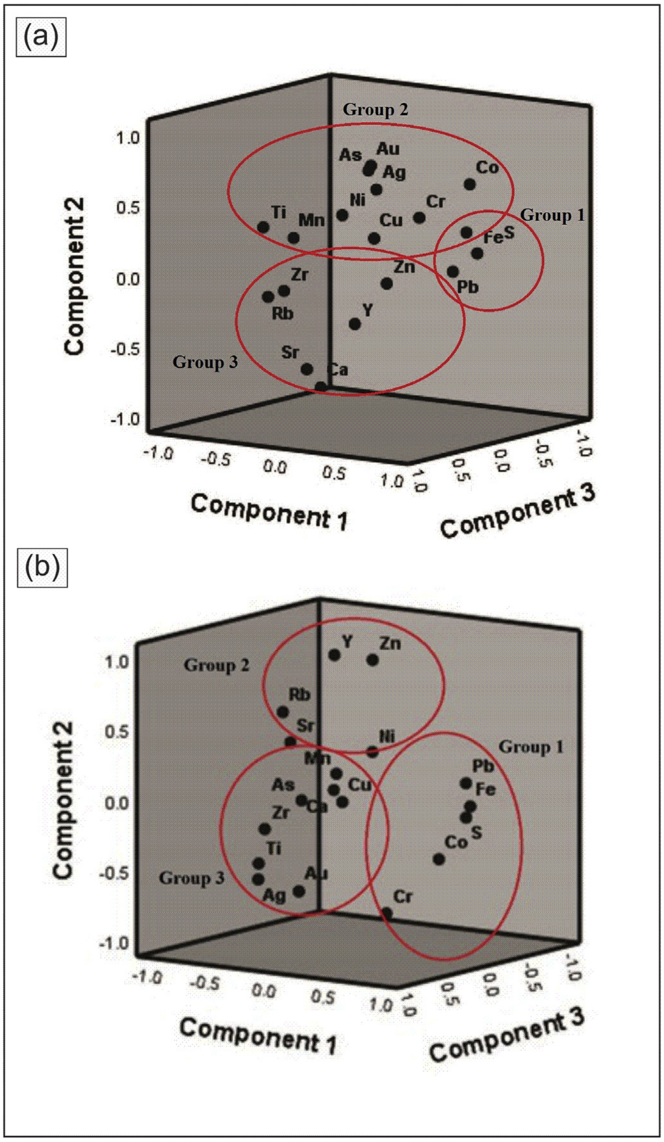

Fig. 6. (a) Factor analysis plot of the untransformed dataset rotated in space, and (b) Factor analysis plot of the transformed dataset rotated in space.

5.2. Constraints from trace element geochemistry

Anomalous concentrations of the elements Fe, Co, and Cr in the laterites are evidence for the presence of mafic volcaniclastic rocks as the parent rocks of the laterites in the Kunche area. Also, comparing the concentrations of Fe, Co, and Cr with laterites derived from mafic volcaniclastic rocks elsewhere (Schellmann, 1986; da Costa and Araújo, 1996; Arhin, 2013) confirms the volcaniclastic source of the laterites in the Kunche area. The high concentrations of Pb, S and As detected in the laterites may be related to hydromorphic dispersion from the sulphide-bearing minerals around the gold prospect. The high Fe content in the laterites relative to the high S content also implies more proximal depositional environments of the laterites particularly the ferruginous laterites. This is because Fe and S cycling or accumulation occurs mostly in depositional environments that are Fe-oxide dominated (Valeton et al., 1987; Riedinger et al., 2017). This is supported by the presence of pisoliths and Fe-oxides in the depositional environment. Nonetheless, the expression of Fe and S in the laterites especially the lateritic duricrusts related to the volcaniclastic host rocks in the area, may also suggest the presence of sulfide-bearing minerals such as pyrite which is associated with gold. Au is known to be soluble in water by

Table 6
Total variance explained for untransformed and transformed datasets.

Total variance explained for raw dataset						
Component	Initial Eigenvalues			Extraction Sums of Squared Loadings		
	Total	% of Variance	Cumulative %	Total	% of Variance	Cumulative %
1	5.922	32.901	32.901	5.922	32.901	32.901
2	4.786	26.591	59.492	4.786	26.591	59.492
3	3.110	17.278	76.770	3.110	17.278	76.770
Total variance explained after centered log-ratio transformation						
Component	Initial Eigenvalues			Extraction Sums of Squared Loadings		
	Total	% of Variance	Cumulative %	Total	% of Variance	Cumulative %
1	5.294	97.353	97.353	4.016	22.312	22.312
2	0.143	2.624	99.977	4.909	27.272	49.584
3	0.001	0.019	99.996	2.818	15.653	65.237

creating complex with S (Stefánsson and Seward, 2004; Pirajno, 2009). This implies that the high S content of the laterites as well as the positive correlation between Au and S might be as a result sulphide complexing with Au.

Laterites are generally poor in Ca, K, and P but show elevated concentration of Cr, Co, and Ni (da Costa and Araújo, 1996). However, the studied laterites show relatively high Ca and low Ni contents whereas Cr and Co are moderately enriched in the laterites. The high Ca content is due to the presence of carbonate-bearing rocks like dolostone, which acts as the intratrapean beds (Dantu, 2014) since the volcaniclastic host rocks of the laterites are in contact with meta-sedimentary rocks in the Kunche area (Fig. 1b). The depletion of Ni in the laterites may be as a result of preferential removal by weathering or perhaps low Ni concentration of the parent rocks. Moderate Cr concentration in the laterites imply Cr enrichment under prevailing pH-redox conditions (Sultan and Shazili, 2009). High concentration of Co in the laterites may be related to the presence of ferromagnesian minerals in the parent rocks (Mitchell, 1964). Ti is relatively stable under denuding conditions but in lateritic settings it can be mobile due to the interplay of geochemical processes (Cornu et al., 1999), therefore its content in the laterites is a signature of weathered remnants of the host rock. The relatively high As content may represent a dispersion halo around gold mineralization in the Kunche area as a result of the nearby gold prospect and the small scale mining activities dotted around the study area. Au and Ag concentrations are relatively high and may be because of complex geochemical processes. During the process of laterization in the warm tropical climate of the Kunche area, oxidation may have occurred at the weathering front below the water table that resulted in neutral to acid conditions in the presence of high sulphides (Kesse, 1985). This resulted in lateral dispersion of Au and Ag from the saprocks towards the top of the profile restricted to the lateritic duricrusts and the mottled zones (Butt and Zeegers, 1992). The formation of Au through such processes in the regolith is very common in West Africa like the case of the Ity Mine of Ivory Coast (Béziat et al., 2016; Mathian et al., 2018). Some detrital ferruginous duricrusts and several samples that fall within the depositional environment have high Au concentrations as well as relatively high concentrations for the pathfinders (Pb, Cu, As, Ag). This might be due to enrichment via lateral hydromorphic dispersion from in situ sources as a result of intense weathering and erosion in the area or possibly enrichment as a result of mixing processes that involve non-geogenic sources. Such areas will therefore be misleading during exploration campaigns.

The Mo, Th, Y, Zn, and Sb concentrations are low in the detrital laterites/duricrusts than the residual laterites/duricrusts. This may also be as a result of preferential removal by weathering. A comparison of the concentration of all the analyzed elements with the average chemical composition of the protoliths mainly volcaniclastics with basalt and andesite compositions suggests enrichment than their respective values according to Turekian and Wedepohl (1961) and Vinogradov (1962) (Table 2), confirming the enrichment by hydromorphic processes or some supergene conditions. After normalizing the element concentrations to the average basalt composition in the earth crust (Turekian and Wedepohl, 1961), Pb, S, Cu, Au, As and Ag displayed longer whiskers above their means and the limit of the average basalt composition (Fig. 10a). Similar trend was observed (Fig. 10b) when the element concentrations were normalized to the average andesite composition in the earth crust (Vinogradov, 1962). Clearly, Pb, Cu, S, Au, As and Ag are enriched more than the average basalt and andesite compositions in the earth crust.

5.3. *Identification of pathfinder elements from geochemical associations*

Multivariate geostatistical analysis is an approach widely used to distinguish the sources (whether geogenic and/or anthropogenic) of heavy metals and trace elements in geological materials (Boruvka et al., 2005). Accordingly, Reimann and Filzmoser (2000) stated that regional geochemical data practically never show a normal distribution. On this basis and from the visual plots (Fig. 5), the data for the analyzed elements can be considered as normally distributed. The existence of small kinks or variations of slope for higher concentration values of Fe, Pb, Cu, As, Ag, and Au in the quantile-quantile plots (Fig. 5) suggest the presence of different sets of populations for those elements. Some extreme concentration values appear as separated from the majority of the samples for all the elements of interest, thus they do not appear to be part of a continuous distribution in the quantile-quantile plots (Fig. 5). These high values are termed as outliers and in exploration geochemistry, they might be considered as evidence of mineralization or other rare processes (Zhang et al., 2005). The three associations observed in the principal component analysis and factor analysis suggest positive correlation among the individual elements in each group and a common geogenic source for their evolution. According to Micó et al. (2006), component 1 in the principal component analysis and factor analysis is usually assigned to be the source that reflects geochemical traces of the primary rock of the duricrust (solely geogenic), component 2 is restricted to a mixed source, and component 3 is related to input from wall rocks and detrital sources. From the above premise, it can be established that Fe, Co and Cr which are associated with component 1 (centered log-ratio transformed data) in our study were sourced directly from the mafic host rocks but S and Pb may be enriched by other sources such as dissolution of sulphide-bearing minerals. Pb does not appear to be a good discriminating pathfinder element in the suite of samples studied due to its weak positive correlation ($r = 0.11$) with Au (Table 4), but should be included as a pathfinder for possible gold-related Cu–Pb–As–Ag mineralization in the Kunche area.

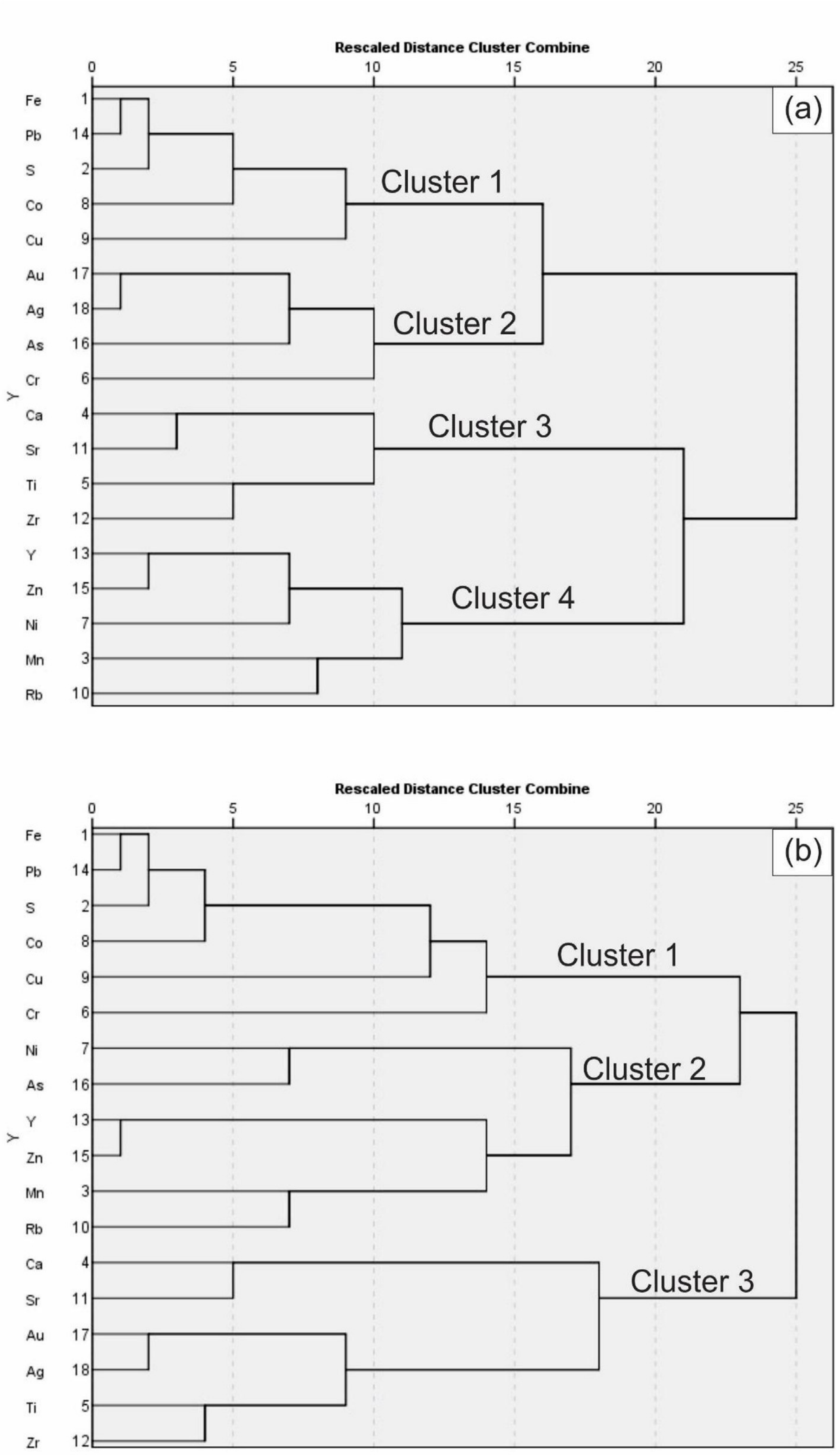

Fig. 7. (a) Dendrogram using average linkage (within groups) indicating four groups of clusters for the untransformed dataset, (b) Dendrogram using average linkage (within groups) indicating three groups of clusters for the transformed dataset.

The relationship is better understood by the influx of chemical sediments as well as the intrusion of magnesium-rich outcrops termed Gondites in the Kunche area (Nude et al., 2012). Component 2 elements mainly Ni, Rb, Sr, Y, and Zn are without a clear distinction of source; they could be input from the wall rocks or supergene sources and are thus usually referred to as contributions of both the igneous protoliths and detrital sources. It is believed that their strong correlation (Table 4) relates to geochemical processes releasing and concentrating these elements, scavenging the elements during laterization and diluting them during intermixing of transported sediments from diverse sources with in-situ regolith materials (Arhin, 2013). Component 3 elements (Ca, Cu, Mn, Ti, Zr, As, Au, Ag) may be input from mainly wall rocks

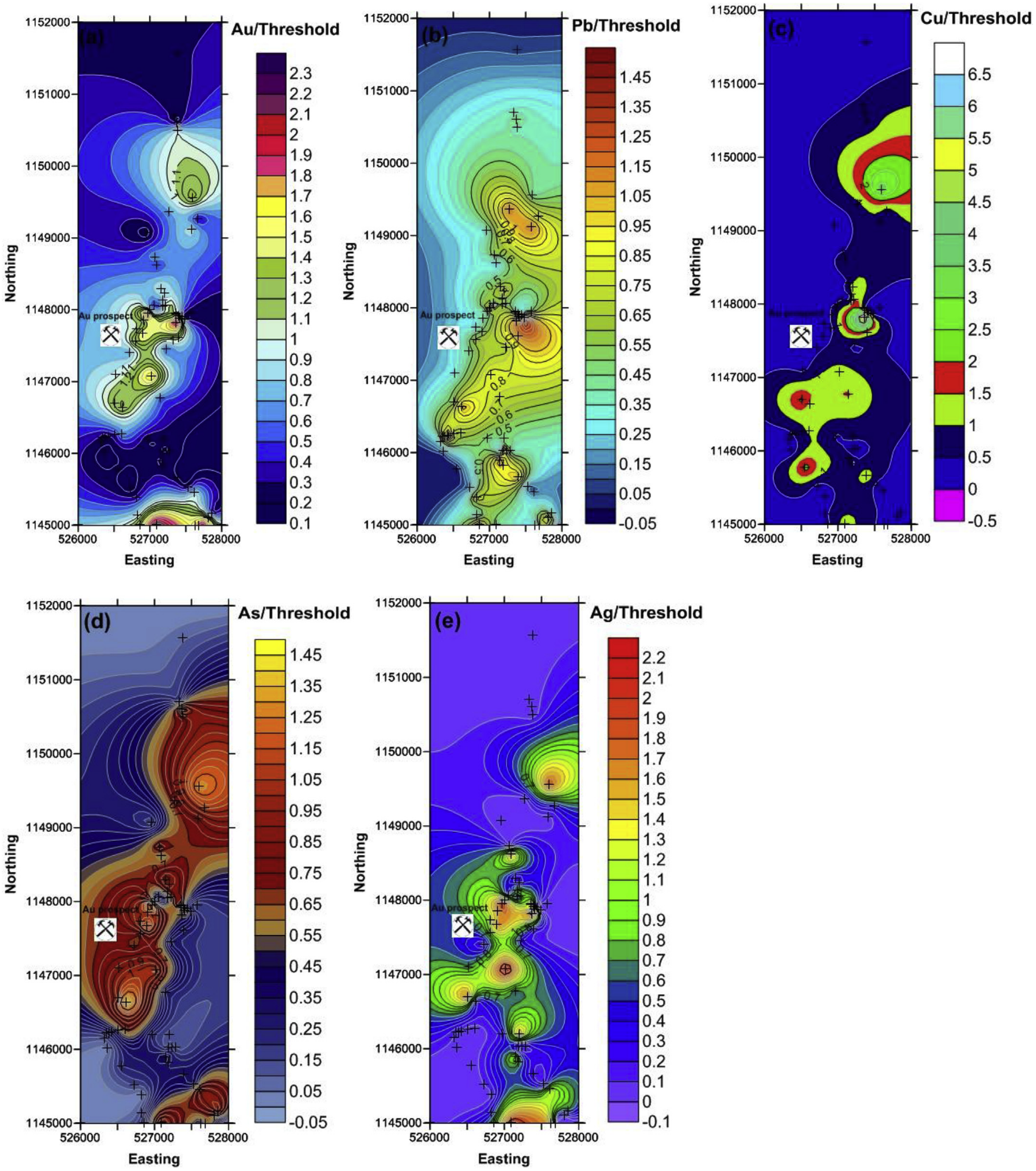

Fig. 8. Single element contour diagrams (using raw concentrations/threshold) showing geochemical anomalies for pathfinder elements in delineating exploration targets (a) Au, (b) Pb, (c) Cu, (d) As, and (e) Ag. The ellipsoidal anomalies above 1 indicated with bold lines are the target areas proposed for exploration programs in Kunche area.

and detrital sources according to Micó et al. (2006). The strong association of Ti with Zr in component 3 of the factor analysis clearly suggests the presence of zircon and anatase as accessory minerals (typical of laterite profiles) whose structures classically contain the elements Zr, Ti, and some REEs (da Costa and Araújo, 1996). Perhaps this elemental association implies the accumulation of zircon and anatase in the regolith profile of Kunche since both elements accumulate under similar conditions in laterites. Zeegers and Lecomte (1992) documented evidence of leaching of most trace elements especially Cu, Zn, Cd, and Ag in the regolith of savannah regions. They stated that some trace elements such as Cu, As and Ag are concentrated in Fe-rich zones. Therefore, the association of Cu, As and Ag with component 2 may be

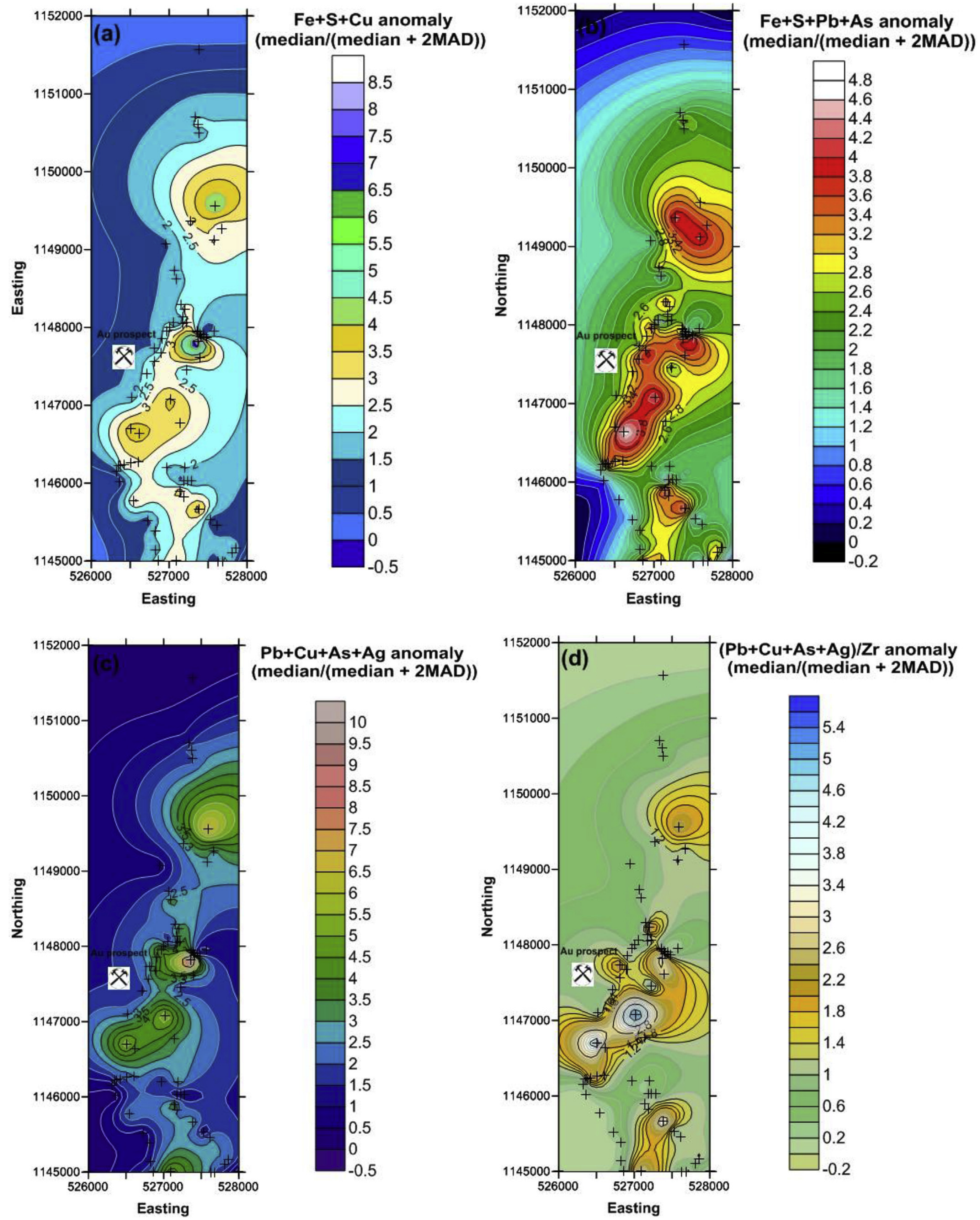

Fig. 9. Prospective gold areas defined by multi-element mapping (median/threshold) (a) Fe + S + Cu, (b) Fe + S + Pb + As, (c) Pb + Cu + As + Ag, and (d) (Pb + Cu + As + Ag)/Zr. The ellipsoidal anomalies above 1 indicated with bold lines are the target areas proposed for exploration programs in Kunche area. (For interpretation of the references to colour in this figure legend, the reader is referred to the Web version of this article.)

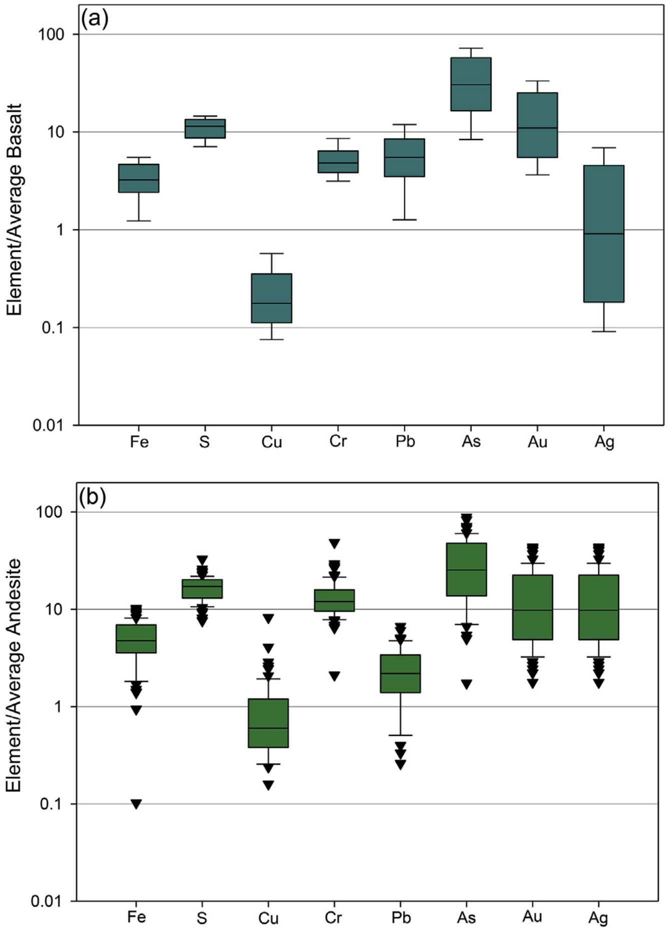

Fig. 10. (a)–(b) Box and whisker plots of selected elements (Fe, S, Cu, Cr, Pb, As, Au, Ag) normalized to the average basalt (Turekian and Wedepohl, 1961) and andesite composition (Vinogradov, 1962) of the earth crust. Dash lines in the boxes are the means whereas the solid lines represent the median.

due to intense weathering, differential erosion, deposition of eroded sediments, and the wide range of geochemical processes acting on them. Generally, Au is an immobile element but it is usually dispersed in the regolith as a mineral complex or sometimes transported as detrital grains by surface processes, hence its association with component 3. Accordingly, the three major associations found in the laterites represent the two likely most abundant mineral groupings: hematite + goethite and anatase + zirconium with kaolinite as the principal clay mineral. They are generally common in both residual and detrital laterites, but are more widespread in the residual laterites.

It is clear that the results of the principal component analysis, factor analysis and hierarchical cluster analysis agree strongly with one another and imply that the occurrence of gold deposits in the Kunche area is directly associated with secondary dispersion of the underlying host rocks containing these elements and laterization. The clusters (Fe, S, Pb, Co, Cu), (Cr, As, Au, Ag), (Ca, Ti, Sr, Zr), and (Mn, Ni, Rb, Y, Zn) in the dendrogram (Fig. 7a) produced from hierarchical cluster analysis of the untransformed data indicate that the first and second clusters are the most homogenous and robust pairs since they have moderate to high concentrations in the lateritic samples. However, after the centered log-ratio (clr) transformation, the clusters obtained (Fe, Pb, S, Co, Cr-cluster 1; Ni, Rb, Sr, Y, Zn-cluster 2; Ca, Cu, Mn, Ti, Zr, As, Au, Ag-cluster 3) (Fig. 7b) suggest that the third cluster is the most homogenous group based on the concentrations of the elements in this group.

Our study confirms that Pb, Cu, As and Ag can also be used in lateritic context, as it can be hypothesized from the works of McQueen et al. (2003) and Reith et al. (2005). The researchers mentioned that Pb, Cu, As, and Ag are known to behave like Au in orogenic belts and thus, are the best pathfinder elements of Au identified in the studied laterites. That accounted for the positive correlations between these elements and Au in the Spearman correlation (Table 4). On bivariate plots involving Au against Cu, Pb, As, and Ag, it is observed that these elements display a direct positive relationship with Au (Fig. 11). Therefore, the Au–Cu, Au–Pb, Au–As, and Au–Ag correlations seem to be primarily controlled by the Au content and strongly serve as pathfinder elements for Au in the Kunche area. Conversely, Zn is not enriched with the identified pathfinder elements despite minor occurrence of sphalerite as an ore mineral in the Kunche area. This is because Zn minerals degrade and usually disperse as host rocks weather to form the regolith (Butt and Zeegers, 2015). The lateritic horizons in the Kunche area with Zn values represent breaks in volcanic activity that produced the volcaniclastic parent rocks and during this time, hydrothermal processes affecting the parent rocks may result in limited accumulation of sulphide minerals like sphalerite. A decrease in hydrothermal activity alongside high pH under reducing conditions, enables Zn to form low solubility complexes with hydroxides and carbonates (Brookins, 1989). Therefore, Zn mobility is hindered in the area resulting in the below detection limit of Zn in most of the studied laterite samples. Moreover, Zn displays negative correlation with Au in the Spearman correlation (Table 4) and can thus be misleading if identified as a pathfinder element of Au in the Kunche area. The identified pathfinder elements also overlap with those recently documented by Anand et al. (2019) in auriferous ferricrete of the Yilgarn Craton of Western Australia and those of Nude et al. (2014) in the regolith of the Tetteh Gold Prospect in the Sefwi Birimian Belt, Southwestern Ghana.

5.4. Exploration implications

The residual laterites/duricrusts are directly related to their formation environment. Their mode of formation, composition and distribution is directly associated with the underlying bedrock composition. In conducting geochemical surveys in an exploration program, sampling residual laterites/duricrusts will give a geochemical signature that represents the sampling environment (Smith et al., 1987). For the detrital laterites/duricrusts, the source materials originate from detached slabs and patches of different duricrust blocks cemented together by clay minerals. They are formed in depositional environments (mixed environments) or lateritic pediments and transitional terrains. Materials found in such environments have erratic compositional properties. They do not have direct relation to their environment of formation. Sampling these laterites in a geochemical survey will not give the underlying geochemical signature of the sampling environment (Anand, 2001). The anomalous zones are predominantly located within the residual laterites (northeastern and central parts). These zones are mainly restricted to the hills and plateaus in the Kunche area (Fig. 12) and thus, we recommend that exploration programs should be focused along those areas. However, the contour diagrams also reveal some geochemical anomalies along some portions of the detrital ferruginous laterite zones (southeastern part) in the Kunche area (Figs. 8 and 9). This may suggest possible enrichment via lateral hydromorphic dispersion of the pathfinder elements from the residual laterites (northeastern and central parts) into the detrital laterites due to weathering. Therefore, such areas might be misleading during mineral exploration and should be avoided. In all, our findings can be compared with similar research conducted by (Mazzucchelli and James, 1966). These researchers demonstrated the presence of a 180 m wide arsenic (As) dispersion halo around gold mineralization in the indurated ferruginous layer of a laterite profile, and in soils derived from the laterite. Therefore, our approach can be considered a proven one for delineating gold exploration targets in laterite capped terrains such as Kunche area in the Wa-Lawra greenstone Birimian belt and the adjacent Bole-Nangodi belt.

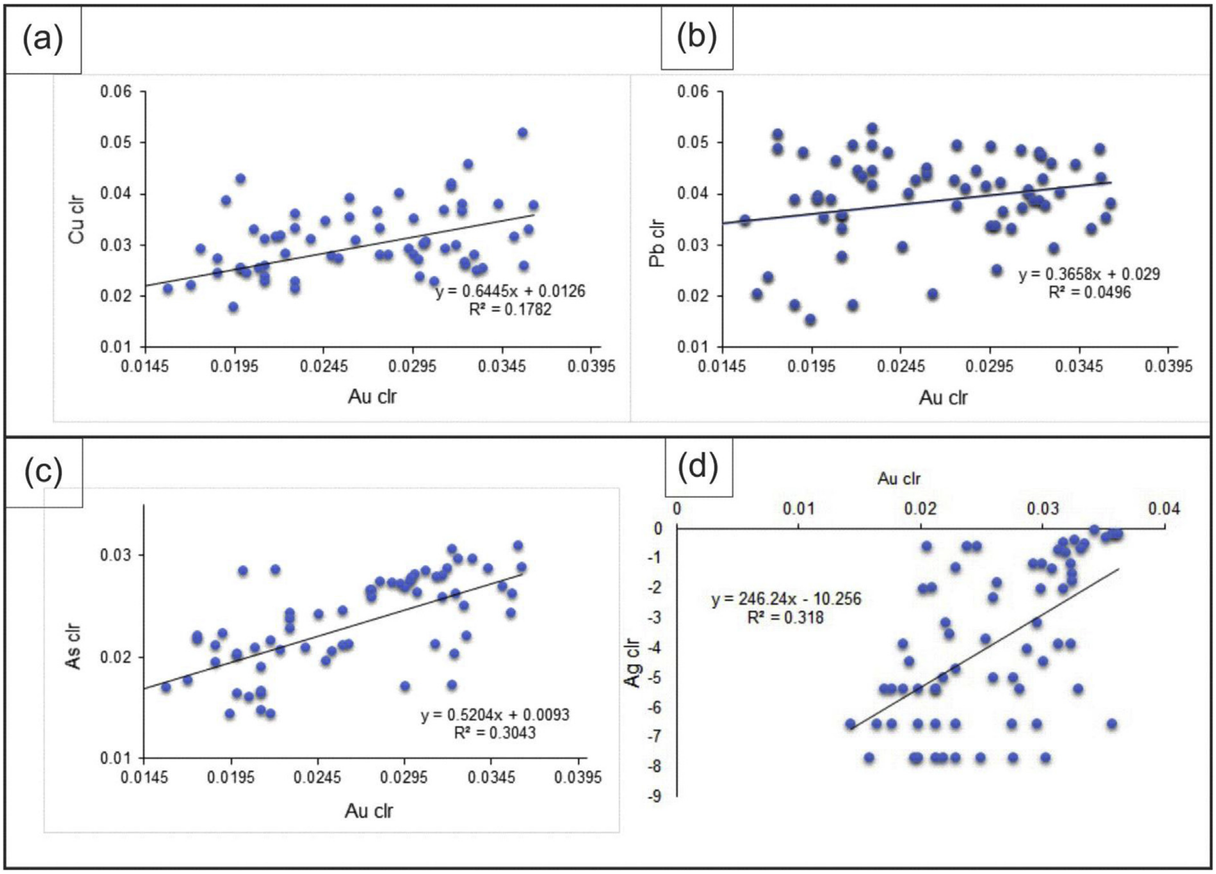

Fig. 11. Bivariate plots of Au and important pathfinder elements (clr = centered log-ratio).

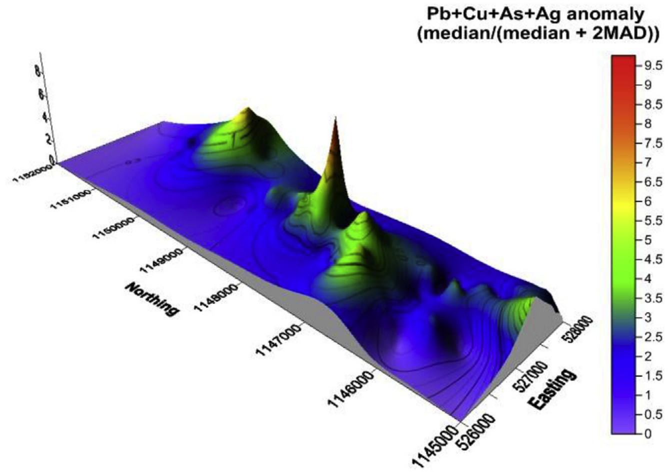

Fig. 12. 3D model showing anomalous areas (hills and plateaus) on the surface of the study area using the median/(median +2MAD) values of the most ideal multi-element association (Pb + Cu + As + Ag).

6. Conclusions

The following conclusions are drawn from the current study;

- ✓ The studied laterites range from detrital laterites (detrital ferruginous duricrust) to residual laterites (lateritic duricrust) and are hosted in volcaniclastic rocks.
- ✓ Geostatistical analysis indicates three element associations; (1) Fe, Pb, S, Co, Cr; (2) Ni, Y, Rb, Sr, Zn; (3) Ca, Cu, Mn, Ti, Zr, As, Au, Ag, which may be due to three factors; mainly the underlying volcanoclastic host rocks and sulphide-bearing deposits, mixed sources, and from wall rocks.
- ✓ The element associations imply that the occurrence of sulfide-bearing deposits such as gold in the Kunche area is directly associated with secondary dispersion of the underlying host rocks and laterization.
- ✓ The important pathfinder elements of gold identified in the laterites are Pb, Cu, As, and Ag since they correlate positively with Au but careful consideration should be given to S during exploration programs due to its high content in the laterites and positive correlation with Au.
- ✓ Single element and multi-element contour diagrams reveal ellipsoidal anomalies that suggest dispersion and accumulation of the pathfinder elements around the northeastern, central, and southeastern parts of Kunche area in close proximity to the gold prospect in the area.
- ✓ The geochemical anomalies are mainly restricted to areas dominated by the residual laterites (northeastern and central parts) on hills and plateaus, hence we recommend gold prospecting in those areas which are increasingly enriched in the pathfinder elements to minimize waste of resources.

Supplementary Tables containing summary statistics of the geochemical data for the lateritic and detrital duricrusts can be accessed online from:https://data.mendeley.com/datasets/bxnwzmm3cw/draft?a=a2397ee4-bdde-42cf-9c88-27604e38e43a.

Acknowledgements

Azumah Resources Limited, Ghana is acknowledged for the support during the period of this research. Special thanks goes to Assoc. Prof. Emmanuel ARHIN at the University for Development Studies, Ghana for his useful comments. The first author thanks TÜBİTAK, BIDEB 2215 Graduate Scholarship Program for International Students for the continuous support as a doctoral research fellow in Turkey. The second author also acknowledges the support from the Graduate Scholarship Program for International Students of the University of Electronic Science and Technology of China. The Editor-in-Chief (Dr. Damien Delvaux), Dr. David Baratoux and other anonymous reviewers are greatly acknowledged for their useful comments that improved the quality of the paper.

Appendix A. Supplementary data

Supplementary data to this article can be found online at https://doi.org/10.1016/j.jafrearsci.2019.103519.

References

Aitchison, J., 1986. The Statistical Analysis of Compositional Data. Chapman and Hall, London, UK, pp. 416.

Aitchison, J., Greenacre, M., 2002. Biplots of compositional data. J. R. Stat. Soc.: Ser. C Appl. Stat. 51 (4), 375–392.

Aleva, G.J.J., 1994. Laterites. Concepts, Geology, Morphology and Chemistry. ISRIC, Wageningen compiler.

Allibone, A., Hayden, P., Cameron, G., Duku, F., 2004. Palaeoproterozoic gold deposits hosted by albite and carbonate-altered tonalite in the chirano district, Ghana, West Africa. Econ. Geol. 99 (3), 479–497. https://doi.org/10.2113/99.3.479.

Amponsah, P.O., Salvi, S., Béziat, D., Siebenaller, L., Baratoux, L., Jessell, M.W., 2015. Geology and geochemistry of the shear-hosted Julie gold deposit, NW Ghana. J. Afr. Earth Sci. 112, 505–523.

Anand, R.R., 1998. Distribution, classification and evolution of ferruginous materials over greenstones on the Yilgarn Craton– implications for mineral exploration. In: Eggleton, R.A. (Ed.), The State of the Regolith. Proceedings of the Second Australian Conference on Landscape Evolution and Mineral Exploration. Conference Publications, Springwood, New South Wales, pp. 175–193.

Anand, R.R., 2001. Evolution, classification and use of ferruginous regolith materials in gold exploration, Yilgarn Craton, Western Australia. Geochem. Explor. Environ. Anal. 1, 221–236.

Anand, R.R., Butt, C.R.M., 2010. A guide for mineral exploration through the regolith in the Yilgarn Craton, Western Australia. Aust. J. Earth Sci. 57 (8), 1015–1114.

Anand, R.R., Hough, R.M., Salama, W., Aspandiar, M.F., Butt, C.R.M., Gonzalez-Alvarez, I., Metelka, V., 2019. Gold and pathfinder elements in ferricrete gold deposits of the Yilgarn Craton of Western Australia: a review with new concepts. Ore Geol. Rev. 104, 294–355. https://doi.org/10.1016/j.oregeorev.2018.11.003.

Anand, R.R., Paine, M., 2002. Regolith geology of the Yilgarn Craton, western Australia: implications for exploration. Aust. J. Earth Sci. 49 (1), 3–162.

Anand, R.R., Wildman, J.E., Varga, Z.S., Phang, C., 2001. Regolith evolution and geochemical dispersion in transported and residual regolith–Bronzewing gold deposit. Geochem. Explor. Environ. Anal. 1 (3), 265–276.

Araújo, E.S., 1994. Geoquimica multi-elementar de crostas e solos lateriticos da AmazBnia Oriental. Ph.D. Dissertation. Federal University of Para, Belem, pp. 241.

Arhin, E., Nude, P.M., 2009. Significance of regolith mapping and its implication for gold exploration in northern Ghana: a case study at tinga and Kunche. Geochem. Explor. Environ. Anal. 9, 63–69.

Arhin, E., 2013. Use of Regolith Geochemistry to Delineate Gold Mineralisation under Cover: a Case Study in the Lawra Belt, NW Ghana. Department of Geology, University of Leicester, UK, pp. 286 (unpublished PhD thesis).

Arhin, E., 2014. Regolith Geochemistry and Hidden Deposits. Lambert Academic Publishing, 978-3-659-59183-9pp. 269.

Arhin, E., Jenkin, G.R., Cunningham, D., Nude, P., 2015. Regolith mapping of deeply weathered terrain in savannah regions of the Birimian Lawra Greenstone Belt, Ghana. J. Geochem. Explor. 159, 194–207.

Beus, A.A., Grigorian, S.V., 1977. In: Levinson, A.A. (Ed.), Geochemical Exploration Methods for Mineral Deposits. Applied Publishing Ltd., Moscow, pp. 280.

Beauvais, A., Colin, F., 1993. Formation and transformation processes of iron duricrust systems in tropical humid environment. Chem. Geol. 106 (1-2), 77–101.

Béziat, D., Siebenaller, L., Salvi, S., Chevalier, P., 2016. A weathered skarn-type mineralization in Ivory Coast: the Ity gold deposit. Ore Geol. Rev. 78, 724–730.

Borůvka, L., Vacek, O., Jehlička, J., 2005. Principal component analysis as a tool to indicate the origin of potentially toxic elements in soils. Geoderma 128 (3-4), 289–300.

Bowell, R.J., 1992. Supergene gold mineralogy at Ashanti, Ghana: implications for the supergene behaviour of gold. Mineral. Mag. 56, 545–560.

Brookins, D.G., 1989. Aqueous geochemistry of rare earth elements. Rev. Mineral. Geochem. 21 (1), 201–225.

Butt, C.R.M., 2016. The development of regolith exploration geochemistry in the tropics and sub-tropics. Ore Geol. Rev. 73, 380–393. https://doi.org/10.1016/j.oregeorev.2015.08.018.

Butt, C.R.M., Bristow, A.P.J., 2013. Relief inversion in the geomorphological evolution of sub-Saharan West Africa. Geomorphology 185, 16–26.

Butt, C.R.M., Zeegers, H. (Eds.), 2015. Regolith Exploration Geochemistry in Tropical and Subtropical Terrains, vol. 4 Elsevier.

Butt, C.R.M., Zeegers, H., 1992. Regolith Geochemistry in Tropical and Sub-tropical Terrains, vol. 4 Elsevier, Amsterdam.

Carter, P., 1997. Wa Reconnaissance License, Terminal Report Prepared for the Minerals Commission Ghana, Ashanti- AGEM Alliance Internal Report.

Chardon, D., Grimaud, J.L., Beauvais, A., Bamba, O., 2018. West African lateritic pediments: landform-regolith evolution processes and mineral exploration pitfalls. Earth Sci. Rev. 179, 124–146.

Colin, F., Vieillard, P., Amborsi, J.P., 1993. Quantitative approach to physical and chemical gold mobility in equatorial rainforest lateritic environment. Earth Planet. Sci. Lett. 114, 269–285.

Cornelius, M., Smith, R.E., Cox, A.J., 2001. Laterite geochemistry for regional exploration surveys–a review, and sampling strategies. Geochem. Explor. Environ. Anal. 1 (3), 211–220.

Cornu, S., Lucas, Y., Lebon, E., Ambrosi, J.P., Luizão, F., Rouiller, J., Neal, C., 1999. Evidence of titanium mobility in soil profiles, Manaus, central Amazonia. Geoderma 91 (3–4), 281–295.

da Costa, M.L., Araújo, E.S., 1996. Application of multi-element geochemistry in Au-phosphate—bearing lateritic crusts for identification of their parent rocks. J. Geochem. Explor. 57 (1–3), 257–272.

da Costa, M.L., Leite, A.S., Pöllmann, H., 2016. A laterite-hosted APS deposit in the Amazon region, Brazil: the physical-chemical regime and environment of formation. J. Geochem. Explor. 170, 107–124. https://doi.org/10.1016/j.gexplo.2016.08.015.

Dantu, S., 2014. Spatial distribution and geochemical baselines of major/trace elements in soils of Medak district, Andhra Pradesh, India. Environ. Earth Sci. 72 (4), 955–981.

Davis, J.C., 1986. Statistics and Data Analysis in Geology, second ed. John Willey & Sons, New York, pp. 646.

Dzigbodi-Adjimah, K., 1993. Geology and geochemical patterns of the Birimian gold deposits, West Africa. J. Geochem. Explor. 47 (1–3), 305–320.

Eggins, S.M., Woodhead, J.D., Kinsley, L.P.J., Mortimer, G.E., Sylvester, P., McCulloch, M.T., Hergt, J.M., Handler, M.R., 1997. A simple method for the precise determination of ≥ 40 trace elements in geological samples by ICP-MS using enriched isotope internal standardisation. Chem. Geol. 134 (4), 311–326.

Eggleton, R.A. (Ed.), 2001. The Regolith Glossary: Surficial Geology, Soils and Landscapes. National Capital Printing, Canberra.

Freyssinet, P., 1993. Gold dispersion related to ferricrete pedogenesis in South Mali: application to geochemical exploration. Croquet de la Recherché Meniere 510, 25–40.

Freyssinet, P.H., Butt, C.R.M., Morris, R.C., Plantone, P., 2005. Ore Forming Processes Related to Lateritic Weathering. Economic Geology One Hundredth Anniversary Volume 1905–2005. SEG, Colorado.

Griffis, R.J., Barning, K., Agezo, F.L., Akosah, F.K., 2002. Gold Deposits of Ghana. Minerals Commission, Accra, Ghana, pp. 438.

Hirdes, W., Davis, D.W., Eisenlohr, B.N., 1992. Reassessment of Proterozoic granitoid ages in Ghana on the basis of U/Pb zircon and monazite dating. Precambrian Res. 56 (1), 89–96.

Ilyas, A., Kashiwaya, K., Koike, K., 2016. Ni grade distribution in laterite characterized from geostatistics, topography and the paleo-groundwater system in Sorowako, Indonesia. J. Geochem. Explor. 165, 174–188. https://doi.org/10.1016/j.gexplo.2016.03.002.

Junner, N.R., 1935. Gold in the Gold Coast 47. Ghana Geological Survey.

Kesse, G.O., 1985. The Mineral and Rock Resources of Ghana. Balkema, Rotterdam.

Loder, T.C., Lyons, W.B., Murray, S., McGuinness, H.D., 1978. Silicate in anoxic pore waters and oxidation effects during sampling. Nature 273 (5661), 373.

Marker, A., Oliveira, J.J., Schellmann, W., 1994. Litho dependence of partly transported weathering horizons above a migmatite-diabase contact in Central Bahia State, Brazil. Catena 21, 215–227.

Mathian, M., Hebert, B., Baron, F., Petit, S., Lescuyer, J.L., Furic, R., Beaufort, D., 2018. Identifying the phyllosilicate minerals of hypogene ore deposits in lateritic saprolites using the near-IR spectroscopy second derivative methodology. J. Geochem. Explor. 186, 298–314.

Mazzucchelli, R.H., James, C.H., 1966. Arsenic as a guide to gold mineralization in laterite covered areas of Western Australia. Inst. Min. Metall. Trans. 75, 286–294.

McQueen, K.G., Munro, D.C., Roach, I.C., 2003. Weathering-controlled Fractionation of Ore and Pathfinder Elements at Cobar, NSW. Advances in Regolith. CRC LEME, pp. 296–300.

Micó, C., Peris, M., Recatala, L., Sanchez, J., 2006. Assessing heavy metal sources in agricultural soils of a European Mediterranean area by multivariate analysis. Chemosphere 65 (5), 863–872.

Mitchell, R.L., 1964. In: Bear, F.E. (Ed.), Chemistry of the Soil Chp. 8. Van Nostrand Reinhold, New York.

Muriithi, F.K., 2015. Centerd log-ratio (clr) transformation and robust principal component analysis of long-term NDVI data reveal vegetation activity linked to climate processes. Climate 3, 135–149.

Nahon, D., Tardy, Y., 1992. The ferruginous laterites. In: Handbook of exploration geochemistry, vol. 4. Elsevier Science BV, pp. 41–55.

Norrish, K., Hutton, J.T., 1969. An accurate X-ray spectrographic method for the analysis of a wide range of geological samples. Geochem. Cosmochim. Acta 33 (4), 431–453.

Nude, P.M., Arhin, E., Foli, S.M.Y.G., Dowuona, G.N., 2014. Geochemical dispersion of elements and their correlation with gold in the regolith at the Tetteh prospect of the chirano gold mines in the Sefwi belt of the Birimian, Southwestern Ghana. J. Environ. Earth Sci. 4 (9), 1–17.

Nude, P.M., Asigri, J.M., Yidana, S.M., Arhin, E., Foli, G., Kutu, J.M., 2012. Identifying pathfinder elements for gold in multi-element soil geochemical data from the Wa-Lawra belt, northwest Ghana: a multivariate statistical approach. Int. J. Geosci. 3 (01), 62.

Pirajno, F., 2009. Hydrothermal processes and wall rock alteration. In: Hydrothermal

Processes and Mineral Systems. Springer, Dordrecht, pp. 73–164.

Reimann, C., Filzmoser, P., 2000. Normal and lognormal data distribution in geochemistry: death of a myth. Consequences for the statistical treatment of geochemical and environmental data. J. Environ. Geol. 39, 1001–1014.

Reis, A.P., Sousa, A.J., Cardosa Fonseca, E., 2001. Soil geochemical prospecting for gold at Marrancos (Northern Portugal). J. Geochem. Explor. 73, 1–10.

Reith, F., McPhail, D.C., Christy, A.G., 2005. Bacillus cereus, gold and associated elements in soil and other regolith samples from Tomakin Park Gold Mine in southeastern New South Wales, Australia. J. Geochem. Explor. 85 (2), 81–98.

Riedinger, N., Brunner, B., Krastel, S., Arnold, G.L., Wehrmann, L.M., Formolo, M.J., Lyons, T.W., 2017. Sulfur cycling in an iron oxide-dominated, dynamic marine depositional system: the Argentine continental margin. Front. Earth Sci. 5, 33. https://doi.org/10.3389/feart.2017.00033.

Schellmann, W., 1986. On the geochemistry of laterites. Chem. Erde 45, 39–52.

Smith, A.J., Henry, G., Frost-Killian, S., 2016. A review of the Birimian Supergroup-and tarkwaian group-hosted gold deposits of Ghana. Episodes 39 (2), 177–197.

Smith, R.E., Perdrix, J.L., Davis, J.M., 1987. Dispersion into pisolitic laterite from the Greenbushes mineralized Sn-Ta pegmatite system, Western Australia. J. Geochem. Explor. 28 (1), 251–265.

Stefánsson, A., Seward, T.M., 2004. Gold (I) complexing in aqueous sulphide solutions to 500 C at 500 bar. Geochem. Cosmochim. Acta 68 (20), 4121–4143.

Sultan, K., Shazili, N.A., 2009. Distribution and geochemical baselines of major, minor and trace elements in tropical topsoils of the Terengganu River basin, Malaysia. J. Geochem. Explor. 103, 57–68.

Sunkari, E.D., Zango, M.S., 2018. Preliminary investigation of the geologic controls of Graphite mineralization and exploration potential of the wa-lawra belt: implications for Kambale Graphite deposit. J. Environ. Earth Sci. 77–89 ISSN 2224-3216 (Paper) ISSN 2225-0948 (Online) 8(3).

Sunkari, E.D., Zango, M.S., Korboe, H.M., 2018. Comparative analysis of fluoride concentrations in Groundwaters in northern and southern Ghana: implications for the contaminant sources. Earth Syst. Environ. 2 (1), 103–117.

Taylor, G., Eggleton, R.A., 2001. Regolith Geology and Geomorphology. John Wiley & Sons, pp. 375.

Taylor, G.F., Thornber, M.R., 1992. Gossan and ironstone surveys. In: Butt, C.R.M., Zeegers, H. (Eds.), Regolith Exploration Geochemistry in Tropical and Subtropical Terrains. Elsevier, Amsterdam, pp. 139–202.

Teng, Y., Ni, S., Wang, J., Zuo, R., Yang, J., 2010. A geochemical survey of trace elements in agricultural and non-agricultural topsoil in Dexing area, China. J. Geochem. Explor. 104, 118–127.

Tukey, J.W., 1977. Exploratory Data Analysis. Addison-Wesley, Reading, pp. 506.

Turekian, K.K., Wedepohl, K.H., 1961. Distribution of the elements in some major units of the earth's crust. Geol. Soc. Am. Bull. 72 (2), 175–192.

Valeton, I., Biermann, M., Reche, R., Rosenberg, F., 1987. Genesis of nickel laterites and bauxites in Greece during the Jurassic and Cretaceous, and their relation to ultrabasic parent rocks. Ore Geol. Rev. 2 (4), 359–404.

Vinogradov, A.P., 1962. Average contents of chemical elements in the principal types of igneous rocks of the earth's crust. Geochemistry 7, 641–664.

Waller, C., Franey, N., Hodgson, S., Widenbar, L., 2012. NI-43-101 Technical Report for. Azumah Resources LTD., Wa Gold Project, Ghana, pp. 114.

Yaylalı-Abanuz, G., 2013. Determination of anomalies associated with Sb mineralization in soil geochemistry: a case study in Turhal (northern Turkey). J. Geochem. Explor. 132, 63–74.

Zeegers, H., Lecomte, P., 1992. Seasonally humid tropical terrains (savannas). In: Handbook of Exploration Geochemistry. vol. 4. Elsevier Science BV, pp. 203–240.

Zhang, C., Manheim, F.T., Hinde, J., Grossman, J.N., 2005. Statistical characterization of a large geochemical database and effect of sample size. J. Appl. Geochem. 20, 1857–1874.